Modeling milk production in the lactation period and the effect of feeding frequency on milk production

by

Katharine R. Faulkner

A THESIS SUBMITTED IN PARTIAL FULFILLMENT OF THE REQUIREMENTS FOR THE DEGREE OF

MASTER OF SCIENCE

in

THE FACULTY OF GRADUATE AND POSTDOCTORAL STUDIES

(Mathematics)

THE UNIVERSITY OF BRITISH COLUMBIA

(Vancouver)

August 2019

The following individuals certify that they have read, and recommend to the Faculty of Graduate and Postdoctoral Studies for acceptance, a thesis/dissertation entitled:

Modeling milk production in the lactation period and the effect of feeding frequency on milk production

submitted by Katharine R. Faulkner in partial fulfillment of the requirements for the degree of Master of Science in Mathematics.

Examining Committee:

Eric Cytrynbaum, Mathematics
Supervisor

Leah Edelstein-Keshet, Mathematics
Supervisory Committee Member

Neil Balmforth, Mathematics
Supervisory Committee Member

Additional Examiner

Additional Supervisory Committee Members:

Supervisory Committee Member

Supervisory Committee Member

Abstract

Human milk production is controlled by a variety of internal and external factors, including hormones, neurons, suckling stimulus and milk removal. One method for increasing milk production suggested to mothers who want to produce more milk is cluster feeding: splitting one feeding into a cluster of multiple feedings. Phenomenological models have been proposed to describe average weekly milk production rates in dairy cattle, but these models do not take into account the effect of the milk removal schedule used. In this thesis, two ordinary differential equation models for describing milk production and milk removal are presented: Model 1, which assumes a linear rate of milk removal during feeding, and Model 2, which uses physical models of fluid flow through a system of ducts to estimate the rate of milk removal. These models are qualitatively very similar, but Model 2 allows for examination of differences in milk dynamics between alveoli at different depths in the mammary gland. 24 hour milk production was then predicted for each model version using various cluster feeding schedules. Feeding schedules which had the most frequent and regular feedings elicited small increases in milk production during a day compared to less frequent or regular schedules. This small increase in milk production suggests that cluster feeding may not be an effective method of increasing production, as other factors that decrease production, like stress, may override this small effect. More work needs to be done to test these models in order to determine an effective method for increasing milk production.

Lay Summary

Mathematical models of physiological systems allow researchers to gain insights into the system being studied through mathematical analysis, as well as perform experiments via theoretical simulations. In this thesis, two models for human milk production are presented and tested. One method for increasing milk production suggested to mothers who want to produce more milk is cluster feeding, splitting one feeding into a cluster of multiple feedings, so these models were tested using various cluster feeding schedules. Feeding schedules which had more frequent feedings elicited small increases in milk production compared to less frequent schedules. This small increase in milk production suggests that cluster feeding may not be an effective method of increasing production, as other factors that decrease production, like stress, may override this small effect. More work needs to be done to test these models in order to determine an effective method for increasing milk production.

Preface

This thesis is original, unpublished work by the author, K.R. Faulkner.

Table of Contents

List of Tables

List of Figures

1. Introduction

Breastmilk is considered the best source of nutrition for infants and lactation is the process by which milk is produced in and secreted from the mammary gland in the breast (Buckley 2015; Amis 2015). In developing countries, lack of maternal nutrition lead to problems with lactation, but low milk production has become an issue for many mothers in developed countries despite adequate nutrition (Walker 1997; Kent et al. 2012; Hurst 2007). Low milk production is especially prevalent in mothers of preterm infants, who must initiate milk production and continue to produce milk throughout the stress from complications of preterm birth (Fewtrell et al. 2016). In these cases, mothers have access to enough food and supplements to be able to produce milk at full capacity, but struggle to do so. There must then be factors dictating the amount of milk produced other than simply nutrition. Mothers and doctors in the developed world are then interested in methods of increasing milk production, and and such methods continue to be extensively studied (Daly et al. 1996; Dewey 2001; Kent et al. 2012; Marasco 2015; Fewtrell et al. 2016).

There are many methods that have been suggested for increasing milk production, such as herbal or pharmacological treatments to increase prolactin levels (the hormone which stimulates milk production), or increasing skin-to-skin contact between the mother and infant (Kent et al. 2012). One method of increasing production that has been suggested is through manipulation of the feeding schedule—feeding more frequently or clustering feedings may increase milk production (Kent et al. 2012; Daly et al. 1996). This type of feeding schedule reduces the between breastfeeding, possibly allowing for more drainage of the breast, both of which are thought to improve milk production (Kent et al. 2012). To what extent these changes in feeding schedule might help increase production, and why increased drainage and fewer extended periods between feedings increase milk production is not fully understood. The goal of this thesis is then to build a model of lactation that explores possible mechanisms behind increased milk production due to changes in the feeding schedule, and to determine how the feeding schedule can be altered to increase production.

Although milk production has been modeled before, it has been largely phenomenological models of dairy cow lactation that describe how milk production changes over the course of the entire lactation period, from initiation to weaning (Wood 1968; Dijkstra et al. 2010; Ferreira et al. 2015; Dag et al. 2005). These studies have included fitting milk production data to very simple differential equation or statistical models, and explored effects like season of lactation initiation on overall milk production. These models also are made to explain changes in milk production over the course of weeks or months, and cannot explain changes that occur on smaller time scales. To explore different types of feeding schedules, a model must be able to reflect changes in milk production that happen over hours or minutes.

There is also a model of the fluid dynamics of milk removal in a human breast (Negin Mortazavi et al. 2016). In this model, the entire mammary gland was simulated, and suckling patterns within a single feeding studied. This model does not include how milk is produced or how that production is regulated. Lactation is a complicated system that is regulated by multiple different types of factors, including neurological signals, many hormones and external physical stimuli. In order to study milk production, these methods of regulation must be included.

Milk production is initiated and promoted by the hormone prolactin, production of which is controlled and inhibited by the neurotransmitter dopamine secreted from specific neurons in the brain (Grattan 2015; Egli et al. 2010). Regulation of prolactin secretion thus goes through these neurons and any regulators that promote prolactin must inhibit TIDA neuron release of dopamine in order to do so. Infant suckling is an example of a neurological signal that promotes prolactin—as the infant suckles on the nipple, the pressure initiates a neurological signal through activation of mechanosensors (Tay et al. 1996). The hormone oxytocin also plays a role in lactation, but not in production—oxytocin causes myoepithelial cells (a thin layer of muscle cells) surrounding the alveoli to contract, pushing milk out of the breast when suckling begins (Tay et al. 1996). These signals are the basic components of lactation that play an important role in milk production. These components, as well as other factors included in the presented models will be described in more detail in the next section.

Mechanisms that will be explored are based on possible effects of milk aging (Daly et al. 1993). Because prolonged periods between feedings and incomplete drainage of the breast inhibit milk production, the mammary gland may have some way of measuring and responding to milk aging as it accumulates in the breast. It has been proposed that there is a signal that accumulates in milk as it ages and that the milk-producing cells in the mammary gland may respond to this signal (Daly et al. 1993; Schmitt-Ney et al. 2014; Cox et al. 1996; Wilde and Peaker 1990). One culprit for this signal is leukemia inhibiting factor (LIF), which has been implicated in cell cycle signalling pathways in the mammary gland of mice (Schere-Levy et al. 2003; Watson 2006). Whatever the signal may be in humans, it is proposed to have an autocrine (local) signalling effects rather than neurological or hormonal effects (Daly et al. 1996; Kent et al. 2012; Wilde and Peaker 1990). Two possible local effects are considered: milk aging causing mammary cells to become quiescent (not active and with the cell cycle paused), and aging causing apoptosis (programmed cell death) of the mammary cells.

In this thesis, two main models are presented. Model 1 explores the physiological mechanisms behind milk production, specifically the local effects of milk aging on production. Four versions of Model 1 are compared in order to analyze different possible effects that milk aging may have on mammary gland cells. This model considers a single alveolus in the mammary gland that is producing and storing milk. Feeding is modeled with a prescribed, constant rate of milk removal during the tested feeding schedule. Model 2 takes the final version of Model 1 and adds on a fluid dynamics based model of milk removal that takes into account some of the geometry of the mammary gland. With this model, more alveoli can be simulated and the differences between those alveoli explored.

2. Models

Two main categories of models were explored: (1) constant flow rate of milk during feeding, and (2) milk flow rate, derived from Poiseuille's Equation for fluid flow at low Reynold's number and pressure balance in the alveoli. Both of these cases used the same general model to describe the relationship of the hormonal and neurological effects on milk production, as described below in Model 1. Model 2 uses the same foundation model, and uses principles from fluid physics to allow for the consideration of more complex geometries.

2.1. Model 1: Constant milk removal

Milk production is controlled by multiple factors, at various time scales. Milk is produced over the course of hours, and the production rate changes over the course of days (Dijkstra et al. 2010). On the other hand, the tuberoinfundibular dopamine (TIDA) neurons, which are the main neurological source of control for milk production, respond within milliseconds to changes in stimuli. The fast time scale variables include blood hormone levels (prolactin and oxytocin), which respond in minutes, and neural stimuli (dopamine, the suckling signal, and the stretch signal), which respond in milliseconds (Cox et al. 1996). The slow time scale variables include milk production, the fraction of alveolar cells that are active and the amount of alveolar cells, which respond in hours. Figure 2.1 shows the locations of release and action for some of the variables involved in milk production.

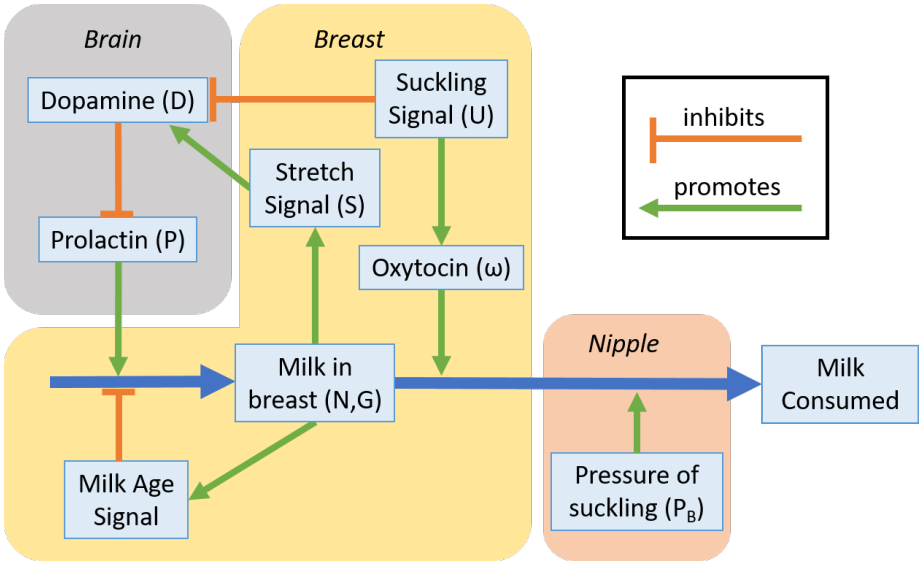

Figure 2.1: Diagram of key variables in milk production with locations in body. Prolactin is produced in the anterior pituitary gland of the brain, and is regulated locally by dopamine released from the TIDA neurons in the pituitary gland. Prolactin is then released into the bloodstream to act at the mammary gland. Stimuli from the breast, including suckling and stretch of the alveoli, travel from the breast to the brain via neurons and the spinal cord.

Fast time scale variables

In this model P represents the level of prolactin, the hormone directly controlling milk production, in the bloodstream. This variable is unitless, corresponding to prolactin concentration relative to the maximum prolactin concentration. Previous models have described prolactin dynamics in non-lactating humans and rats (Rattanakul and Lenbury 2009; Bertram et al. 2006). While some models account for regulation of prolactin by the hormone thyrotropin-releasing hormone (TRH), others consider TRH merely an intermediary step between dopamine regulation and prolactin secretion that can be ignored (Bertram et al. 2006). In Model 1, factors that could only affect TRH were not considered, so for simplicity TRH was not included as a separate variable. Instead the parameters in Equation 1.1a are assumed to be functions of TRH, and all regulation of prolactin secretion is through dopamine.

Prolactin secretion from the posterior pituitary is under perpetual inhibition

from the TIDA neurons in the pituitary, which release dopamine according to the neurons' firing rate, D (normalized to its maximum firing rate so D is unitless). Prolactin is then produced at a rate that decreases as the TIDA neuron firing rate increases. Prolactin also is reabsorbed from the bloodstream at a rate proportional to itself. Similar to the model made by Bertram et al in 2006, the differential equation for prolactin level is

$$\frac{dP}{dt} = \frac{k_{P1}}{k_{P2} + D} - k_{P3}P. \tag{1.1a}$$

The constants k_{P1} and k_{P2} describe dopamine-regulated prolactin production so that k_{P1}/k_{P2} is the maximum prolactin production rate and k_{P2} is the relative TIDA firing rate at which prolactin is produced at half of its maximum rate. The rate of prolactin removal is then k_{P3}. In this model, it is assumed that prolactin levels in the blood equilibriate quickly relative to milk production and feeding (Tay et al. 1996). The right hand side of Equation 1.1a is set to zero and prolactin is at a quasi-steady state described by

$$P = \frac{k_{P1}}{k_{P3}(k_{P2} + D)}. \tag{1.1b}$$

Milk removal is also known to influence milk production, and accumulation of milk could influence production either through stretch on the alveolus cortex or accumulation of a milk aging factor (Wilde and Peaker 1990). The effect of milk aging as a local signal will be discussed in a later section, but the stretching of the alveolus was considered as a potential neurological signal that affects TIDA neuron firing in this model. Additionally, the mechanical suckling on the nipple is known to influence prolactin production, and would also do so through the TIDA neurons (Tay et al. 1996). These signals—stretch and suckling—would be sent via neurons from the breast to the TIDA neurons in the brain, so S is the relative firing rate of neurons carrying the stretch signal and U is the relative firing rate of neurons carrying the suckling signal (each normalized to their respective maximum firing rates, so S and U are unitless). Stretch of the alveoli indirectly decreases prolactin production and therefore promotes TIDA neuron firing. Suckling on the nipple indirectly increases prolactin production, through inhibition of TIDA neuron firing. These two stimuli, stretch and suckling, are assumed to affect TIDA neuron firing independently, with

each sufficient to affect TIDA firing on their own. The differential equation for D, relative TIDA neuron firing, is

$$\frac{dD}{dt} = k_{D1}\left(\frac{1}{k_{D2}+U} + \frac{S}{k_{D3}+S}\right) + k_{D4} - k_{D5}D. \tag{1.2a}$$

Action potentials in the TIDA neurons are then produced at a rate inversely proportional to U and at an additional rate that saturates with S. Because prolactin production is under perpetual inhibition from the TIDA neurons, these neurons must have a constant background action potential production rate k_{D4}. In this model, it is assumed that the firing rate in the TIDA neurons equilibriates quickly relative to milk production and feeding, so the right hand side of 1.2a is set to zero and this firing rate is at a quasi-steady state described by

$$D = \frac{k_{D1}}{k_{D5}}\left(\frac{1}{k_{D2}+U} + \frac{S}{k_{D3}+S}\right) + \frac{k_{D4}}{k_{D5}}. \tag{1.2b}$$

The firing rate for the suckling signal, U, is produced only when the infant is suckling and is assumed to decay away rapidly after suckling stops. The equation for the suckling signal firing rate is then

$$U = k_U f(t), \tag{1.3}$$

where $f(t)$ is a characteristic function for the feeding schedule, with $f = 1$ during feeding and $f = 0$ otherwise. The parameter k_U is the fixed firing rate during suckling. The stretch signal, S, is a saturating function of stress on the membrane, σ,

$$S = \frac{k_{S1}\sigma}{k_{S2}+\sigma}. \tag{1.4}$$

For the constant milk removal case, the stress was assumed to be directly related to the amount of milk in the alveolus, N, with $\sigma = k_\sigma N$.

Finally, during feeding, high oxytocin levels in the blood, ω, causes the myoepithelial cells around the alveoli to contract, squeezing milk out of the mammary gland by generating a pressure on the alveoli whose role is described later (Tay et al. 1996). As with prolactin, ω is normalized to the maximum oxytocin concentration level and ω is unitless. The suckling signal causes this rise in oxytocin, and the differential equation for oxytocin is

$$\frac{d\omega}{dt} = k_{\omega 1}U - k_{\omega 2}\omega. \tag{1.5a}$$

The suckling signal firing rate produces oxytocin with a constant rate $k_{\omega 1}$ and decays away with constant rate $k_{\omega 2}$. In this model, it is assumed that oxytocin equilibriates quickly relative to milk production and feeding, so the right hand side of Equation 1.5a is set to zero and oxytocin is at a quasi-steady state described by

$$\omega = \frac{k_{\omega 1}}{k_{\omega 2}} U = \frac{k_{\omega 1}}{k_{\omega 2}} k_U f(t). \tag{1.5b}$$

Slow time scale variables

Four variations of Model 1 were considered in order to explore different possible mechanisms for the effect of aged milk on production. Because milk aging has been found to be an autocrine (local) signal, it must affect the cells producing milk directly (Wilde and Peaker 1990; Schmitt-Ney et al. 2014). Two possible age signals which could affect milk production are leukemia-inhibiting factor (LIF) and serotonin, both of which are local signals in the mammary gland which have been shown to be important for involution, the termination of milk production after feeding ends (Schere-Levy et al. 2003; Horseman and Collier 2013).

Two possible mechanisms for such an age signal were considered: the age signal deactivating alveolar cells, with the cells left occupying space in the alveolus and not producing milk, but capable of being recruited to produce milk again; and the age signal causing apoptosis of alveolar cells, which are then removed or shed, decreasing the size of the alveolus. Each combination of these two mechanisms was explored, including the case where neither exists and milk aging has no effect.

No milk age signal

With no age signal, all molecules in the milk were treated as the same and tracked collectively as N, the number of moles of "dry" (non-water) milk molecules in the alveolus. This milk is produced at a rate that depends on both the serum prolactin level, P, and the number of productive cells surrounding the alveolus, which is related to the reference (non-stretched) radius of the alveolus, r_0, and the proportion of alveolar cells that are active, C:

$$\frac{dN}{dt} = k_N P C r_0^2 - N\frac{Q}{V} - k_l N, \tag{2.1a}$$

where $V = 4\pi r_0^3/3$ is the total volume of the alveolus and Q is the volumetric flow rate out of the alveolus (both constant in this case, with $Q/V = k_{Fl}$). The milk, N is removed with feeding at rate NQ/V. Milk also leaks out of the alveolus, between gaps in alveolar cells, or is reabsorbed back into the surrounding cells with constant rate k_l.

Milk age affecting cell quiescence

In the case where aged milk does have an effect, it must be tracked separately from new milk as G, the amount of aged milk in moles. New milk, N, is converted to aged milk at some rate k_G, thus modifying the equation for N to include this conversion:

$$\frac{dN}{dt} = k_N PCr_0^2 - N\frac{Q}{V} - k_l N - k_G N, \tag{2.1b}$$

Aged milk has the same rate of removal and leakage as new milk:

$$\frac{dG}{dt} = -G\frac{Q}{V} - k_l G + k_G N. \tag{2.2}$$

If the age signal promotes cell quiescence, but not cell removal, then the number of alveolar cells (and therefore the reference radius) would remain constant. The variable affected would then be the proportion of these cells which are actively producing milk, C. In the absence of an age signal, all cells would be recruited to produce milk, with prolactin acting as an activator of quiescent cells (Horseman and Collier 2013). As age signal accumulates, it would then deactivate cells, decreasing C. The differential equation for C is then

$$\frac{dC}{dt} = k_{C1} P(1 - C) - k_{C2} CG, \tag{2.3}$$

where prolactin activates cells at rate k_{C1}, and the age signal deactivates cells at rate k_{C2}. In this case, the alveolus reference radius, r_0 remains constant.

Milk age affecting alveolus size

If the age signal promotes cell removal, then the number of cells surrounding the alveoli would change, but all the cells would be actively producing milk. The number of cells surrounding the alveolus is proportional to its reference surface area, $4\pi r_0^2$. The number of cells, and therefore the surface area, is assumed to grow logistically with a rate constant that depends on prolactin, leading to the following differential

equation for the radius:

$$\frac{dr_0}{dt} = (k_{r1} + k_{r2}P)r_0(r_{0,max}^2 - r_0^2) - k_{r3}r_0G. \tag{2.4}$$

The cells have a background growth rate of k_{r1}, with a "carrying capacity" or maximum radius $r_{0,max}$, and prolactin increases the growth rate by $k_{r2}P$. The age signal, G, accelerates apoptosis and removal of cells, decreasing the radius with constant rate k_{r3}. In this case, the proportion of alveolar cells that are active, C, would remain constant.

Milk age affecting cell quiescence and alveolus size

If both of the described mechanisms for age signal action are in effect, then neither C nor r_0 would be constant. To test these two mechanisms together, both equations 2.3 and 2.4 were used.

2.2. Model 2: Pressure-based milk removal

In order to explore the effects of including multiple alveoli in a branching structure with this model, as well as to test the hypothesis that differences in milk removal between alveoli in the mammary gland affect milk production, the flow rate out of each alveolus must be determined. These flow rates are dependent on the geometry of the branching, therefore principles from fluid physics are needed to describe the relationship. These principles were applied first to a simple structure with a single alveolus, then to larger branching structures with multiple alveoli.

Flow out of a single alveolus.

To determine the flow rate of milk from a single alveolus, through a duct, and out of the nipple, we invoke Poiseuille's law. According to this law, at low Reynold's number, the flow rate, Q, of fluid through a single pipe is

$$Q = \frac{\pi r^4}{8\nu l}\Delta P, \tag{3.1}$$

where r is the radius of the pipe, l is the length of the pipe, ν is the viscosity of the fluid and ΔP is the change in pressure from one end of the pipe to the other. According to one study, viscosity of breast milk ranges between 1.2×10^{-3} and 2.5×10^{-3} Pa·s (Sunarić et al. 2016). Various duct lengths and radii were tested.

For a single alveolus, the change in pressure across a single pipe is the difference between the pressure from the alveolus, P_A, and the pressure at the nipple from the infant suckling, P_B. The pressure from the infant is prescribed and various values of this pressure were tested. The pressure from the alveolus can be derived from force balance on the alveolus cortex, assuming that the volume of the alveolus equilibriates quickly so that these forces are in balance. This force balance yields the following pressure in the alveolus:

$$P_A = \begin{cases} \frac{Kh}{r_A}\left(\frac{r_A^2}{r_0^2} - 1\right) + P_\omega, & r_A \geq r_0 \\ P_\omega, & r_A < r_0, \end{cases} \tag{3.2}$$

where r_A is the stretched radius of the alveolus, r_0 is again the non-stretched reference radius, and P_ω is some prescribed pressure exerted by the myoepithelial cells surrounding the alveolus as they contract in response to oxytocin during feeding (Newton and Newton 1948). In order to find the stretched radius, r_A, the quasi-steady-state volume equation for a single cell (Jiang and Sun 2013) was modified for an alveolus to include outflow of milk as follows:

$$\frac{dV_A}{dt} = -\beta\left(\Delta P - \Delta\Pi\right) - Q = 0. \tag{3.3}$$

Here, ΔP is the difference in hydrostatic pressure between the interior and exterior of the alveolus ($P_{in} - P_{ex}$), $\Delta\Pi$ is the difference in osmotic pressure between the interior and exterior of the alveolus ($\Pi_{in} - \Pi_{ex}$), and β is a parameter describing the volume of water moved across the membrane per unit pressure change. The difference in hydrostatic pressure, ΔP, is the difference between the alveolus interior pressure, P_A (Equation 3.2), and the contraction pressure, P_ω. The difference is then

$$\Delta P = P_A - P_\omega = \begin{cases} \frac{Kh}{r_A}\left(\frac{r_A^2}{r_0^2} - 1\right), & r_A \geq r_0 \\ 0, & r_A < r_0. \end{cases} \tag{3.4}$$

The osmotic pressure, Π, is related to the concentration of milk in the associated region. The osmotic pressure in the cells surrounding the alveolus, Π_{ex}, is assumed to be constant at pressure Π_C. The difference in osmotic pressures is then

$$\Delta\Pi = \frac{N}{V_A}RT - \Pi_C = \frac{3N}{4\pi r_A^3}RT - \Pi_C, \tag{3.5}$$

where N is the moles of milk inside the alveolus, V_A is the volume of the alveolus, R

is the ideal gas constant, and T is body temperature. The flow out of the alveolus, Q, is related to the difference in pressure between the alveolus, P_A, and the end of the duct leading away from the alveolus. In the case with a single alveolus, this pressure is the pressure from the infant suckling, P_B. Using Poiseuille's Law, Equation 3.1, the flow rate out of the alveolus is

$$Q = \frac{\pi r_d^4}{8\nu l_d}(P_A - P_B) = \begin{cases} \frac{\pi r_d^4}{8\nu l_d}\left(\frac{Kh}{r_A}\left(\frac{r_A^2}{r_0^2} - 1\right) + P_\omega - P_B\right), & r_A \geq r_0 \\ \frac{\pi r_d^4}{8\nu l_d}(P_\omega - P_B), & r_A < r_0, \end{cases} \tag{3.6}$$

where r_d and l_d are the radius and length of the duct between the alveolus and the nipple. We can now use equations 3.4-3.6 to write dV_A/dt in Equation 3.3 as a function of r_A, as follows:

$$0 = \begin{cases} -\beta\frac{Kh}{r_A}\left(\frac{r_A^2}{r_0^2} - 1\right) + \beta\left(\frac{3N}{4\pi r_A^3}RT - \Pi_C\right) - \frac{\pi r_d^4}{8\nu l_d}\left(\frac{Kh}{r_A}\left(\frac{r_A^2}{r_0^2} - 1\right) + P_\omega - P_B\right), & r_A \geq r_0 \\ \beta\left(\frac{3N}{4\pi r_A^3}RT - \Pi_C\right) - \frac{\pi r_d^4}{8\nu l_d}(P_\omega - P_B), & r_A < r_0. \end{cases} \tag{3.7}$$

This equation can then be solved at each time step for r_A using a non-linear solver (`fsolve` in Matlab 2019a, Mathworks). The flow rate, Q, of milk out of the alveolus can then be found using Equation 3.6.

Flow out of multiple alveoli.

In order to determine the flow rate of milk from a collection of alveoli, through a system of ducts, and out of the nipple, a similar process as for a single alveolus is used. To determine the flow rates in a branching network, Poiseuille's law was applied to each section of duct, with conservation of mass applied at junctions between two or more pipes (flow into the junction must equal flow out of the junction). Each alveolus is connected by a duct with radius r_k and length l_k to a main duct with radius $r_{d,k}$ and length $l_{d,k}$ between the k^{th} junction and the next junction ($k+1$ or the nipple). Figure 2.2 shows the branching structure used and the location of each parameter in the scheme.

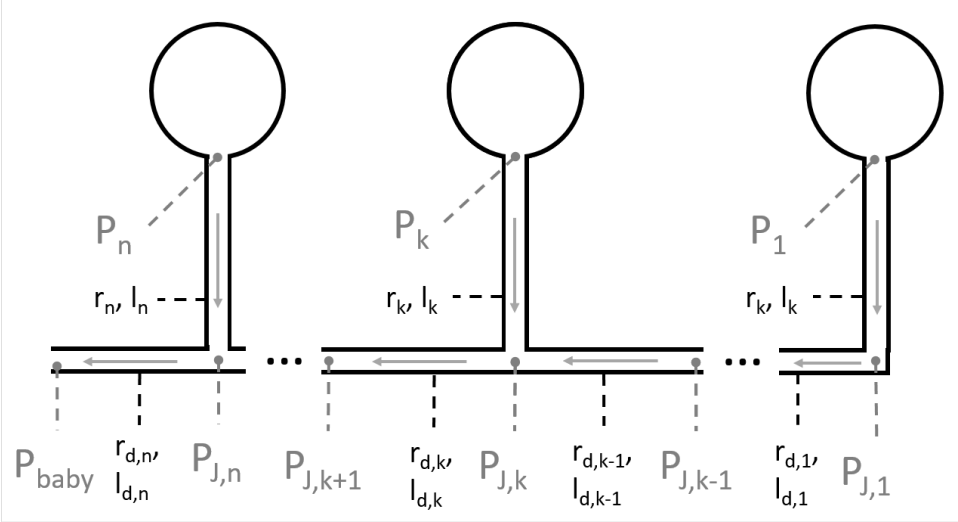

Figure 2.2: Diagram of pressures and duct parameters in branching alveoli network. Black labels indicate prescribed parameters describing the branching network and gray labels indicate pressure values at a point in the network. The lower, horizontal duct is the main duct to the nipple (at the left end of the duct), while the vertical ducts are branches between the alveoli and the main duct. P_{baby} is the pressure at the nipple from infant suckling.

There are now n volume equations, similar to Equation 3.3, and n equations for conservation of mass and flow at each junction between ducts. This system of non-linear equations can then be used to solve for the alveoli radii, $r_{A,k}$, and the pressure at the junctions, $P_{J,k}$, at each time step in order to determine the flow rate, Q_k, out of each alveolus.

Similarly to the single-alveolus case, the volume differential equation is quasi-steady-stated and each term can be rewritten as a function of $r_{A,k}$. With multiple alveoli, the flow rate Q_k will also depend on the junction pressure $P_{J,k}$. Following the same derivation from Equation 3.3 to 3.7, we get from

$$\frac{dV_{A,k}}{dt} = -\beta\left(\Delta P_k - \Delta\Pi_k\right) - Q_k = 0 \tag{3.8}$$

to two cases: if $r_{A,k} \geq r_0$, then Equation 3.8 becomes

$$0 = -\beta\frac{Kh}{r_{A,k}}\left(\frac{r_{A,k}^2}{r_0^2} - 1\right) + \beta\left(\frac{3N_k}{4\pi r_{A,k}^3}RT - \Pi_C\right) - \frac{\pi r_k^4}{8\nu l_k}\left(\frac{Kh}{r_{A,k}}\left(\frac{r_{A,k}^2}{r_0^2} - 1\right) + P_\omega - P_{J,k}\right), \tag{3.9a}$$

and if $r_{A,k} < r_0$, then Equation 3.8 becomes

$$0 = \beta \left(\frac{3N_k}{4\pi r_{A,k}^3} RT - \Pi_C \right) - \frac{\pi r_k^4}{8\nu l_k}(P_\omega - P_{J,k}). \tag{3.9b}$$

There are then n equations (3.9), one for each $k = 1$ to n. To solve for both $r_{A,k}$ and $P_{J,k}$, we need n more equations. In order to conserve mass in the mammary gland duct network, the net flux of milk at each junction of ducts must be zero. For each alveolus, $k = 2, \ldots, n-1$, the net flow through the associated junction is

$$0 = \frac{\pi r_k^4}{8\nu l_k}(P_k - P_{J,k}) + \frac{\pi r_{d,k-1}^4}{8\nu l_{d,k-1}}(P_{J,k-1} - P_{J,k}) - \frac{\pi r_{d,k}^4}{8\nu l_{d,k}}(P_{J,k} - P_{J,k+1}). \tag{3.10a}$$

For the first alveolus, there are only two ducts making up the junction (Figure 2.2), so for this junction, we have

$$0 = \frac{\pi r_1^4}{8\nu l_1}(P_1 - P_{J,1}) - \frac{\pi r_{d,1}^4}{8\nu l_{d,1}}(P_{J,1} - P_{J,2}). \tag{3.10b}$$

Finally for the last alveolus, the duct with milk leaving the junction goes directly to the infant, so the following pressure is P_B, the pressure from infant suckling. For this junction, we then have

$$0 = \frac{\pi r_n^4}{8\nu l_n}(P_n - P_{J,n}) + \frac{\pi r_{d,n-1}^4}{8\nu l_{d,n-1}}(P_{J,n-1} - P_{J,n}) - \frac{\pi r_{d,n}^4}{8\nu l_{d,n}}(P_{J,n} - P_B). \tag{3.10c}$$

The equations 3.9 and 3.10 can be solved simultaneously using a non-linear solver (`fsolve` in Matlab 2019a, Mathworks) at each time step to give the stretched radius, $r_{A,k}$, and junction pressure, $P_{J,k}$, for each alveolus, k.

2.3. Parameter Choices

Parameter values were chosen so that simulations produced physiologically reasonable results. Key characteristics that made a simulation "reasonable" include: all variables remain non-negative (with the exception of pressure values which could be negative) and bounded, variables respond to initiation of feeding at an appropriate speed (quickly for P, D and ω when not in a quasi steady state, and slowly for N, G, C and r_0), milk values decrease during feeding, C and/or r_0 decrease in response to increasing G, and `fsolve` succeeds to solve Equation 3.7 or Equations 3.9a-3.10c at each time-step. All parameter values used are given in the appendix in Tables A.1 and A.2. Unless otherwise stated, all simulations shown in the results use these

parameter values.

3. Results

3.1. Model 1: Constant milk removal

No milk age signal

In this model (Equations 1.1a-2.1a), aged milk is assumed to have no effect on milk production and is thus not tracked separately from new milk. There is then only one slow variable: N, the amount of milk in the alveolus. Figure 3.1 shows a sample milk profile for a single day with feeding once for one hour in every four hours.

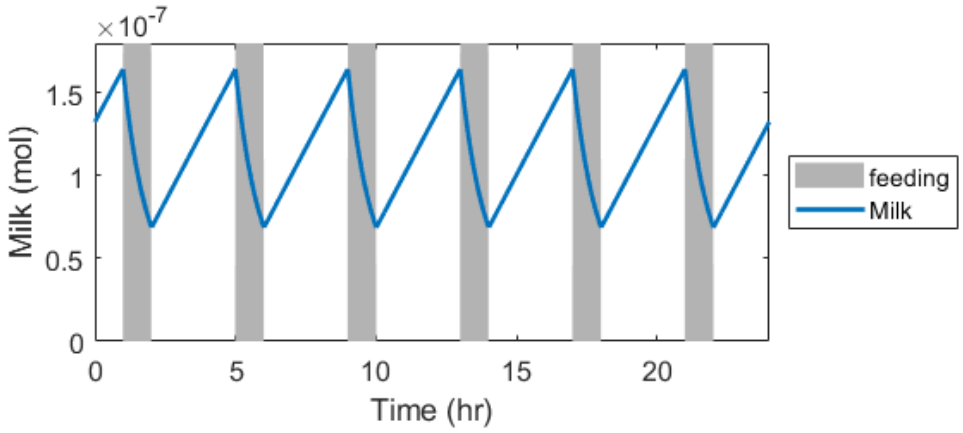

Figure 3.1: Simulated milk curve for 24 hours of feeding one hour in every four, as predicted by Model 1, constant milk removal with no milk aging. Gray regions indicate time periods of feeding.

As expected, the amount of milk oscillates: decreasing during feeding as the infant removes milk and increasing between feedings as milk is produced. While the alveolus does not empty during feeding, it is reduced to less than half of the pre-feeding amount by the end of each feeding. Milk production has balanced so that the amount of milk produced matches the amount that is removed and the system has no overall loss or gain of milk in the alveolus during this day.

Human breastmilk is about 7% lactose by weight, so if we use the molecular weight of lactose (342.3 g/mol) for the "dry" milk (N), this simulation corresponds to about 3.4×10^{-8} g of milk (including water weight) produced in a day (Jenness 1979). Because only a single alveolus is being modeled and the same parameters will be used for both constant removal and pressure-based removal in order to compare the results more directly, this amount of milk produced is much smaller than that of a mammary gland (Kent (2006) found that mothers produced 440 to 1220 g normally in 24 hours). Differences between modeling alveoli of varying sizes will be discussed in a later section.

To investigate the behavior of this model, the dynamics of the milk, N were considered for two cases: between feedings (no milk removal) and during feeding (sustained milk removal). Figure 3.2 shows the phase portrait for N with this model. During a day with multiple feedings, oscillations in the amount of milk are caused by the system jumping between these two cases.

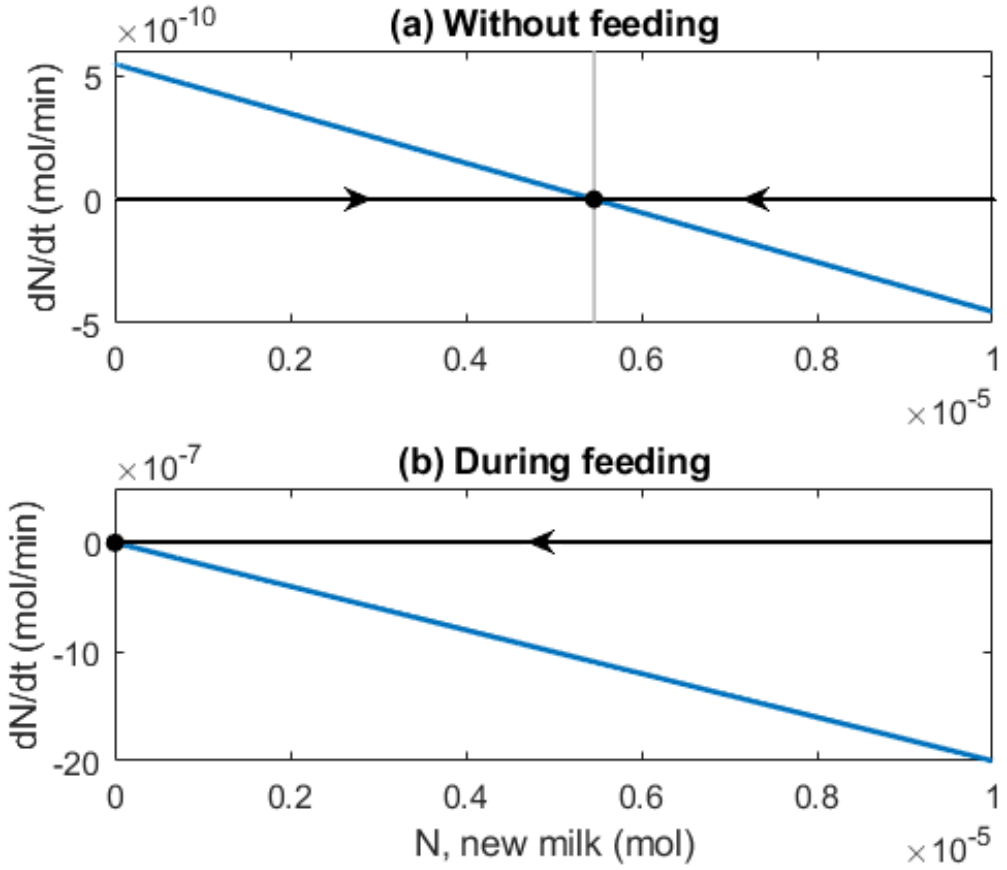

Figure 3.2: Phase lines for Model 1, constant milk removal with no milk aging, and the two system states: (a) between feedings (no milk removal) and (b) during feeding (sustained removal). Between feedings (a), there is a single stable steady state at $N = 5.46 \times 10^{-6}$ mol. With sustained feeding (b), there is a single stable steady state at $N = 2.97 \times 10^{-9}$ mol.

Each case has a single stable steady state, with feeding moving the steady state from a relatively high value of 5.46×10^{-6} mol of milk down three orders of magnitude to a relatively low 2.97×10^{-9} mol. The non-feeding steady state (a) dictates the long-term behavior of the amount of milk after weaning. During the first stage of involution, before structural changes to the mammary gland cause additional milk reabsorption, the system will move towards this value.

Before weaning, the lactation system will oscillate in between these two steady

states, constantly jumping between the two phase lines. Notice that in the sample day of feeding, milk remains between 0.5×10^{-7} and 2×10^{-7} mol—near neither of the two steady states (Figure 3.2).

Although the during feeding equilibrium gives the long-term result of milk in the mammary gland with no feeding, this model can only describe up to two days after feeding ends—through the first stage of involution when production slows. After two days, structural changes occur and leftover milk is reabsorbed, guided by hormonal effects not described in this model (Jindal et al. 2014; Watson 2006). . Figure 3.3 shows milk production during the two days after feeding ends.

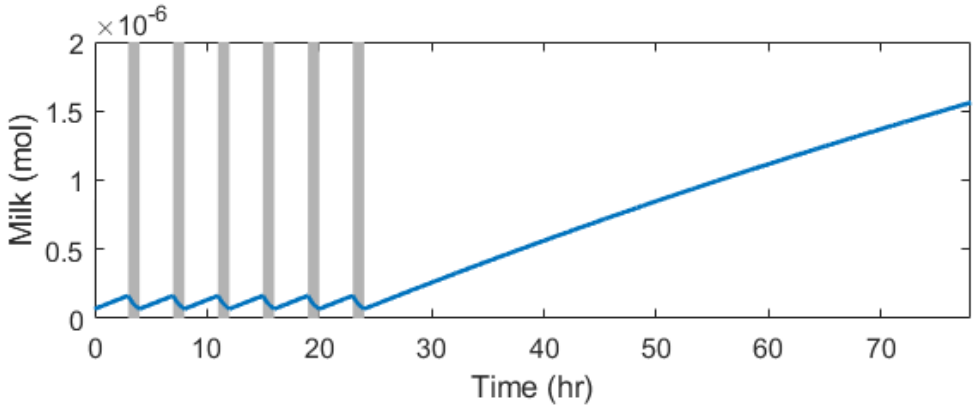

Figure 3.3: Simulated milk curve for the end of feeding, as predicted by Model 1, constant milk removal without milk aging. Periods of feeding are shown in gray and end at hour 24.

After feeding ends, milk rises quickly after the final feeding and is ten times higher by the end of the two days of no feeding. However, milk does not reach the equilibrium point of 5.46×10^{-6} mol during this time frame. In fact, it does not approach this equilibrium until about four weeks after feeding ends, far beyond the scope of this model.

Milk age affecting cell quiescence

In this model, new milk ages and is converted to aged milk, G, and causes alveolar cell quiescence (Equations 1.1a-2.3). There are now three slow variables: N,

new milk, G, aged milk, and C, proportion of alveolar cells active. Figure 3.4 shows a sample day with feeding occurring regularly once in every four hours.

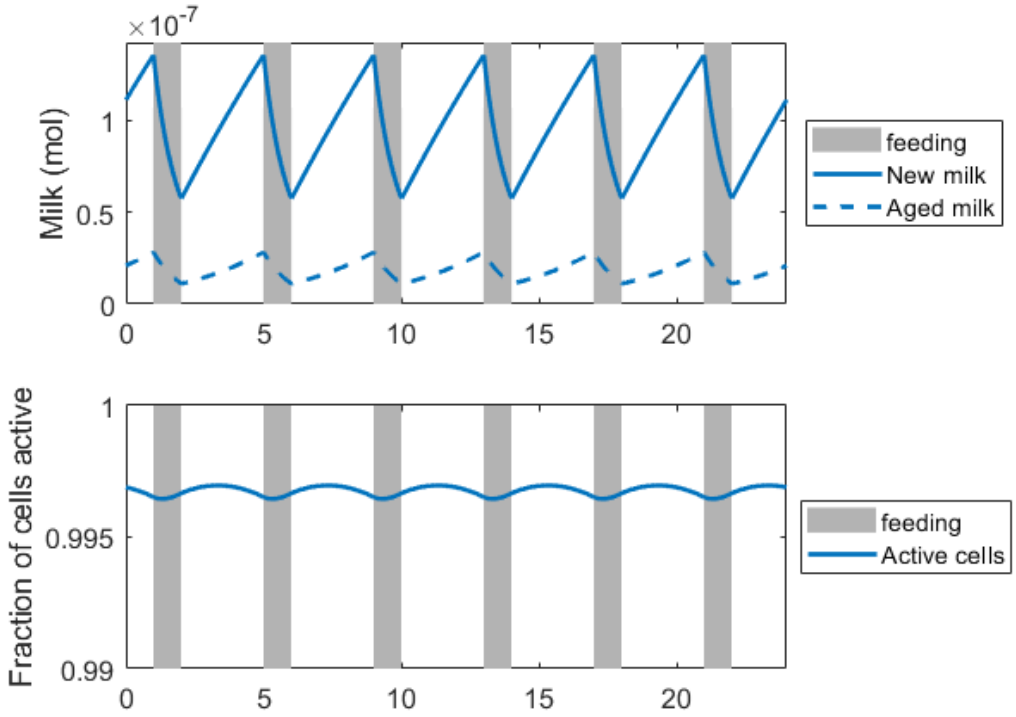

Figure 3.4: Simulated milk curve for 24 hours of feeding one hour in every four, as predicted by Model 1, constant milk removal with aged milk affecting cell quiescence. Gray regions indicate time periods of feeding.

New and aged milk both oscillate, increasing between feedings and decreasing during feeding. The fraction of cells active, however, increases while aged milk is low and decreases when aged milk is sufficiently high, causing oscillations with the same period as for milk. Over all, aged milk is relatively low and the fraction of cells active remains close to one.

Including the effect of milk aging on cell quiescence did not change the daily pattern of milk production during feeding, but it may change milk production during involution. Figure 3.5 shows the lactation system in the two days after the final feeding compared to the last day of feeding.

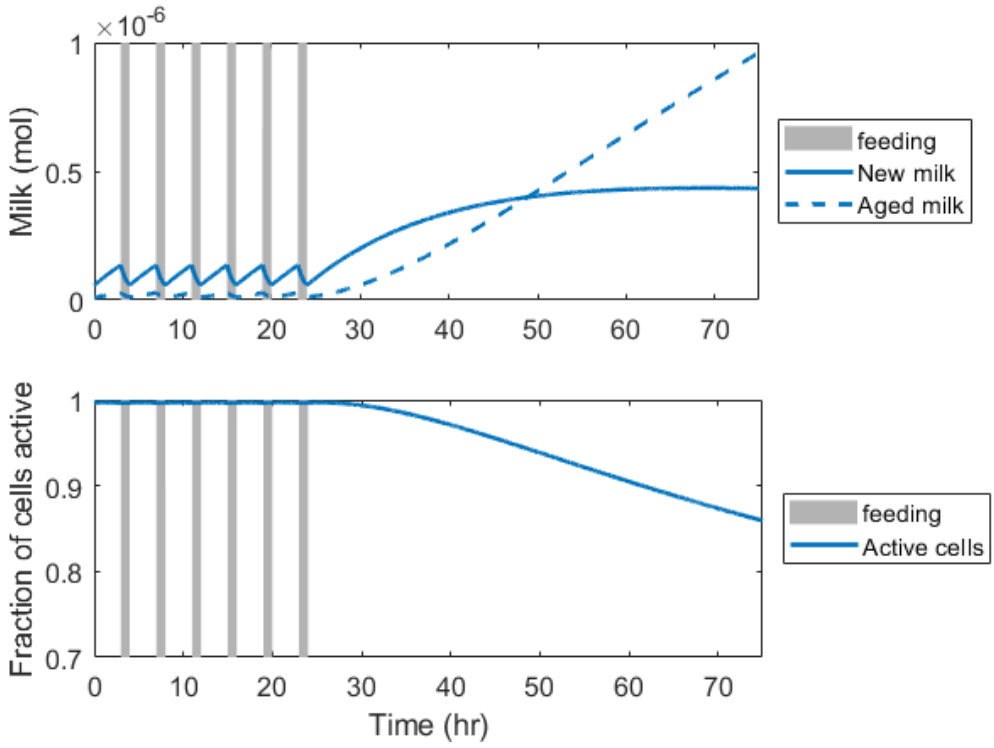

Figure 3.5: Simulated milk curve for the end of feeding, as predicted by Model 1, constant milk removal with aged milk affecting cell quiescence. Periods of feeding are shown in gray and end at hour 24.

In this case, production of new milk slows soon after the final feeding while aged milk production speeds up. By the end of the two days, new milk has leveled off while aged milk continues to grow quickly. The fraction of cells active drops as aged milk rises and continues to decrease steadily to the end of the two day period. Although C decreases slowly and does go below 85% of cells active, this small decrease is sufficient to slow new milk production to matching the rate of aging within the two day involution period.

Milk age affecting alveolus size

In this model, aged milk causes alveolar cell death (Equations 1.1a-1.5b, 2.1b, 2.2, 2.4). The slow variables are then N, G and r_0, the reference (non-stretched) radius of the alveolus. Figure 3.6 shows a sample day of regular feeding with this model.

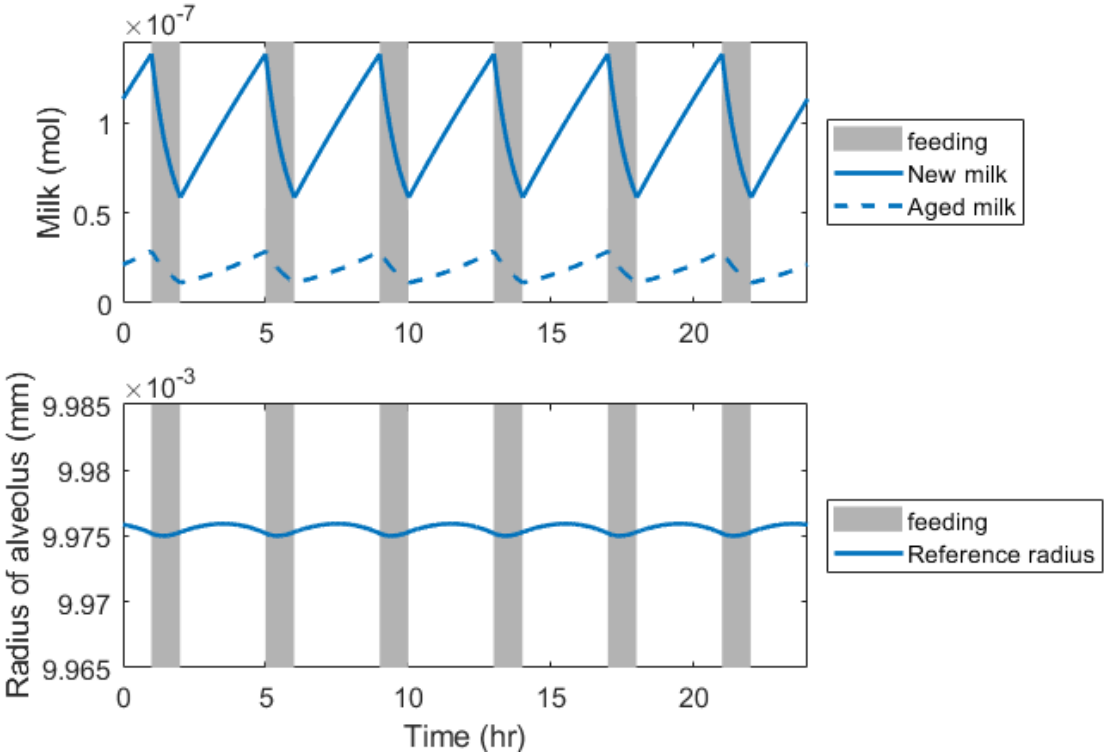

Figure 3.6: Simulated milk curve for 24 hours of feeding one hour in every four, with Model 1, constant milk removal with aged milk affecting alveolus size. Gray regions indicate time periods of feeding.

New and aged milk oscillate similarly to the previous model. The reference radius also oscillates in a similar pattern to C in the previous model—increasing while aged milk is low and decreasing once aged milk is sufficiently high.

Involution also shows similarities between the two models. Figure 3.7 shows the lactation system during involution.

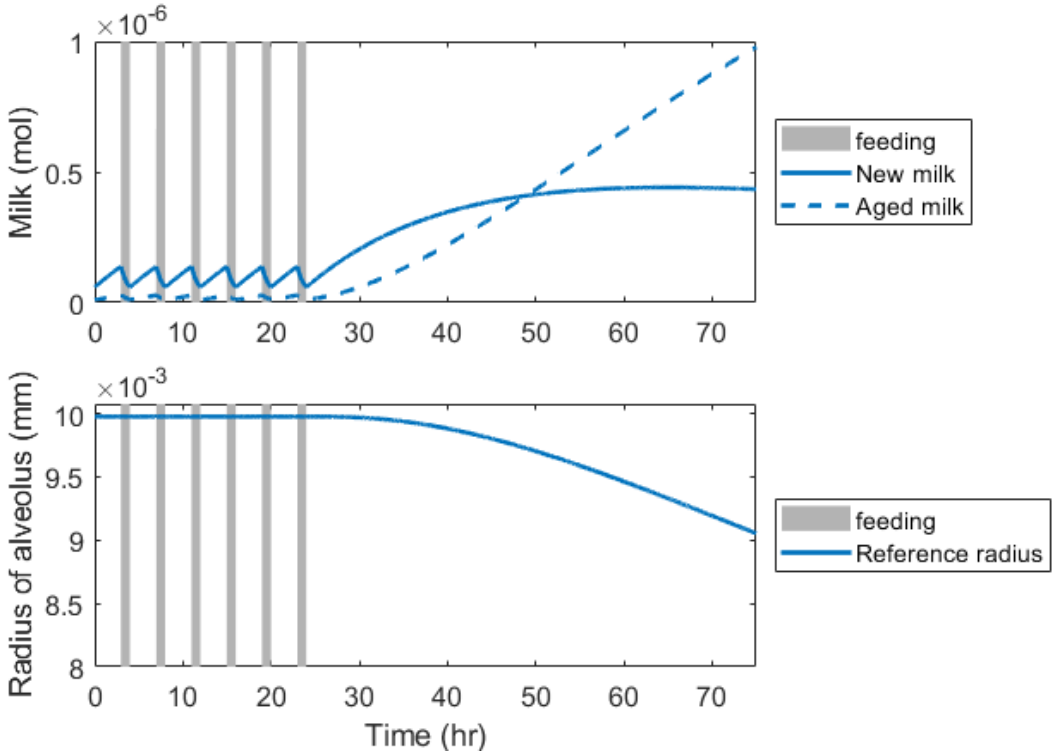

Figure 3.7: Simulated milk curve for the end of feeding, as predicted by Model 1, constant milk removal with aged milk affecting alveolus size. Periods of feeding are shown in gray and end at hour 24.

The alveolus radius decreases later and more gradually after feeding ends than the fraction of cells active decreased. However, the same effect on new and aged milk production is seen: new milk production slows until new milk levels off while aged milk rises rapidly until the end of the period. Additionally, although r_0 decreases more gradually than C, in this case new milk begins to decrease slightly by the end of involution stage one.

Milk age affecting cell quiescence and alveolus size

In this final version of Model 1, aged milk both deactivates alveolar cells and causes alveolar cell death. All four slow variables are in effect: N, G, C and r_0. Figure 3.8 shows a sample day of milk production with regular feeding occurring for one hour in every four hours.

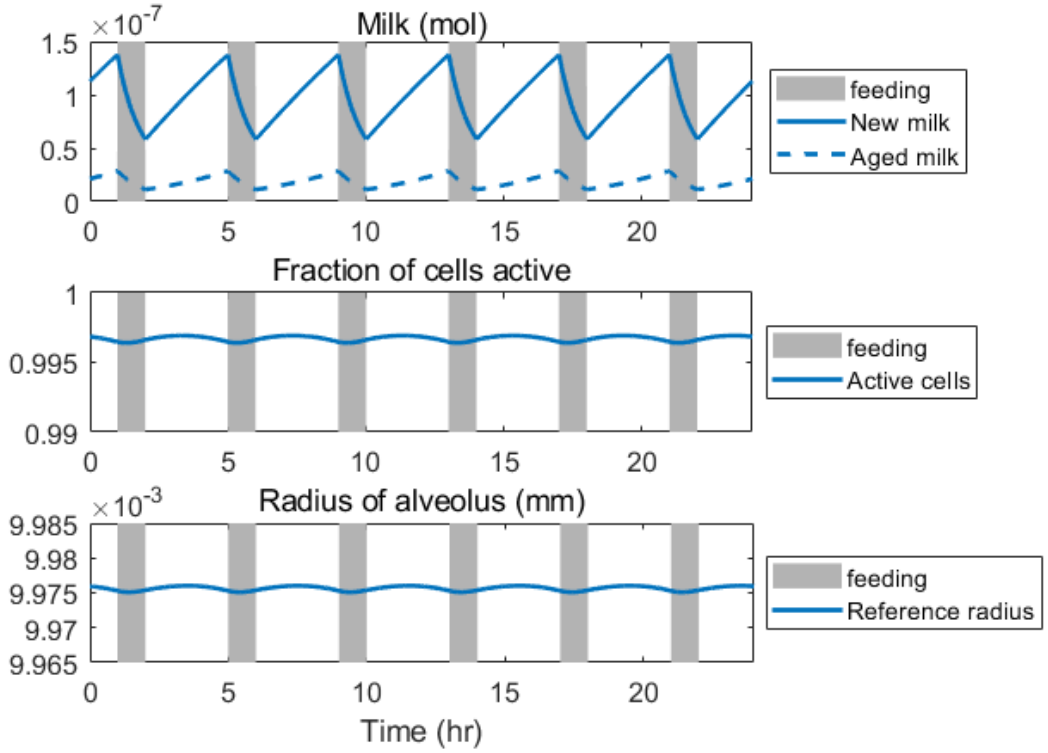

Figure 3.8: Simulated milk curve for 24 hours of feeding one hour in every four, with Model 1, constant milk removal with aged milk affecting cell quiescence and alveolus size. Gray regions indicate time periods of feeding.

When paired together, the effects of milk age on active cells and alveolus radius maintain the same patterns as seen when they were modeled separately. The fraction of cells active still oscillates between 0.995 and 0.999, increasing while aged milk is low and decreasing when it is high (Figure 3.8). Similarly, the reference radius oscillates near 9.97×10^{-3} mm both when it is included alone and with C (Figure 3.8). These oscillations follow the aged milk pattern, which is also maintained. New and aged milk increase between feedings and decrease during feeding, with aged milk oscillating between 1×10^{-8} mol and 3×10^{-8} mol, and new milk oscillating between 5×10^{-8} mol and 1.5×10^{-7} mol (Figure 3.8). Involution also shows similarities between the two models. Figure 3.9 shows the lactation system during involution.

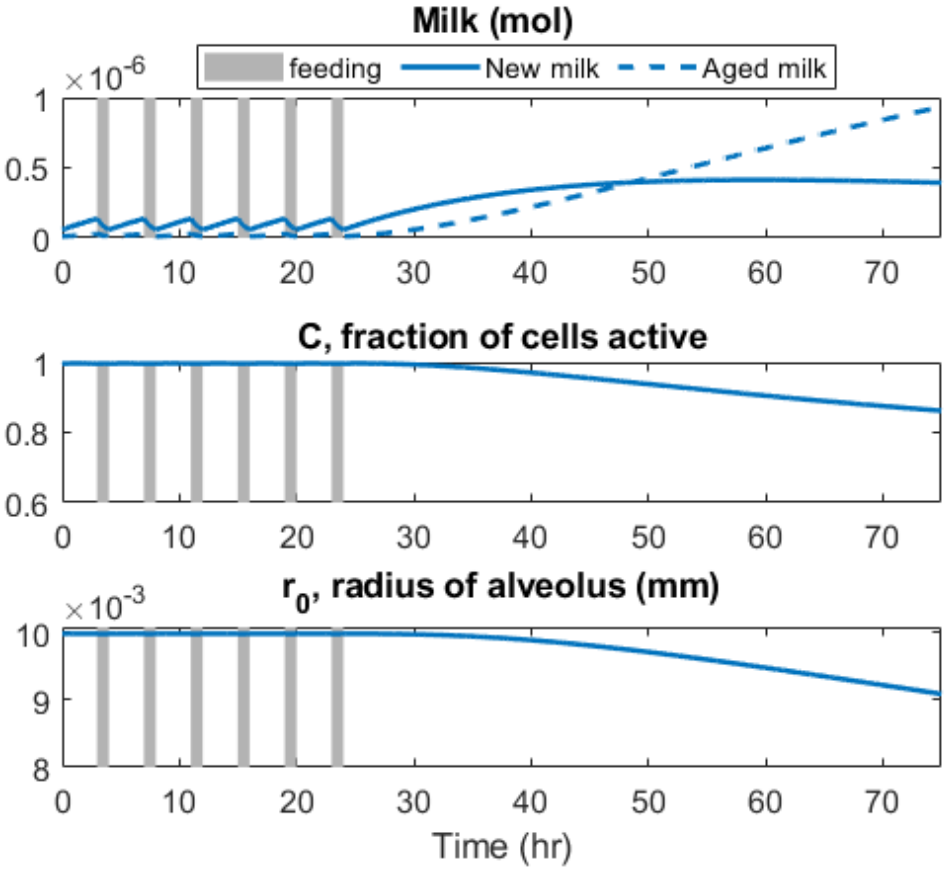

Figure 3.9: Simulated milk curve for the end of feeding, as predicted by Model 1, constant milk removal with aged milk affecting cell quiescence and alveolus size. Periods of feeding are shown in gray and end at hour 24.

Again, the same general patterns are found when the two milk aging effects are paired together. All four versions of Model 1 show similar daily patterns and all show marked increases in milk levels during the first stage of involution, although not including the effects milk aging causes milk to rise fastest after the final feeding. Including the effect of milk aging in any capacity produced similar dynamics in milk production as well as the variables affected by milk age.

Cluster feeding with constant milk removal

Increased frequency of feeding has been shown to increase production in women with low milk supply, so various cluster feeding schedules were tested on each version

of Model 1 and the amount of milk produced compared (Fewtrell et al. 2016; Daly et al. 1996). The previously used feeding schedule of feeding one hour in every four was then modified to test different numbers of feedings in a single cluster. The amount of time spent feeding per period (one hour) and the length of the period (four hours) were maintained, but the hour of feeding was split into N_c feedings 20 minutes apart. Figure 3.10 shows the amount of milk produced for the four constant milk removal models discussed in this section with six different feeding schedules ($N_c = 1$ is the regular feeding schedule used previously, $N_c > 1$ are cluster feeding schedules as described). The amount of milk produced was measured by summing the production component of the N equation (Equation 2.1b) across all time steps.

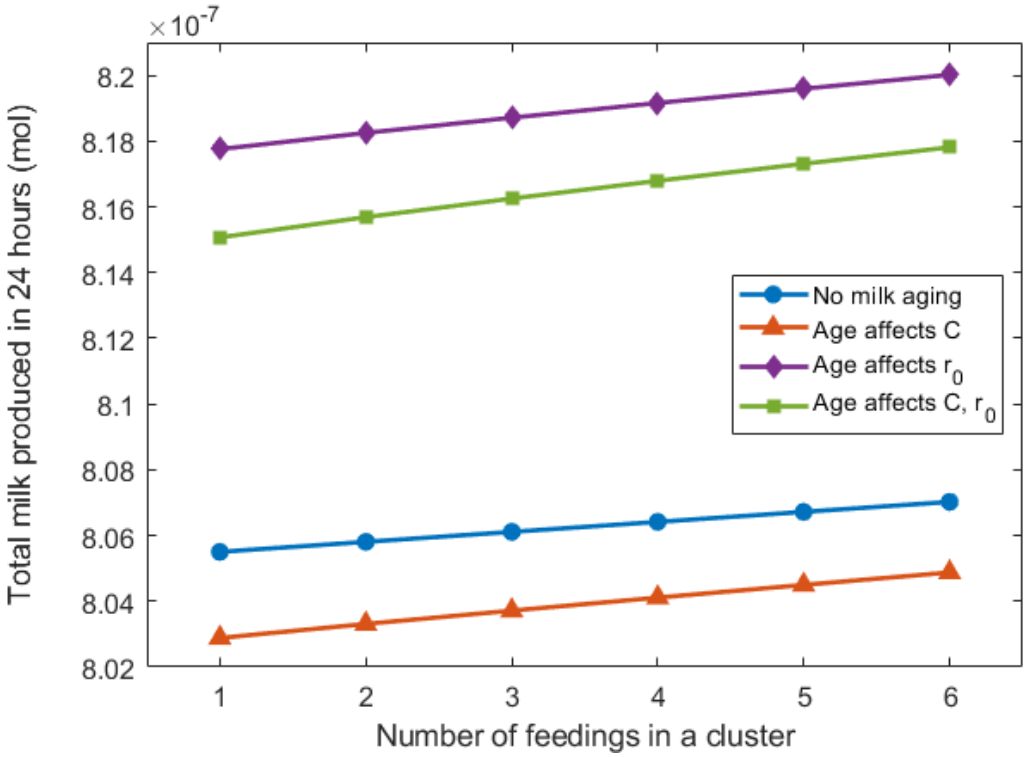

Figure 3.10: Total milk produced in 24 hours for each of the four versions of Model 1, and six different feeding schedules. A single feeding in a cluster ($N_c = 1$) corresponds to a regular feeding schedule with one hour of feeding in every four hours. Higher numbers of feedings in a cluster correspond to one hour of feeding split into N_c feedings, 20 minutes apart, every four hours.

For each model, the amount of milk produced increases with the number of feedings in a cluster, although only slightly. Both versions of the model in which milk aging affects alveolus size (r_0) produce consistently higher milk across all numbers of feeding. Including the effect of milk aging on the proportion of active cells (C) lowers the amount of milk produced. In cases where age affects r_0, the alveolus is allowed to grow in response to low levels of aged milk, generating a higher milk production capacity. In the cases where age affects C, the alveolar cells are allowed to deactivate in response to high levels of aged milk rather than having C fixed at one. Even though including the effect of aged milk on C decreased production, it also increased the system's sensitivity to changes in the feeding schedule, as seen by the differences in slope in the bottom two curves.

Although continuing to increase the number of feedings per cluster at some point generates an entirely impractical feeding schedule, methods of increasing milk production are of interest. Thus the time in between feedings in a cluster, previously fixed at 20 minutes, was varied in order to allow for more feedings in a cluster while keeping the period of the feeding schedule fixed at four hours. Figure 3.11 shows the amount of milk produced in 24 hours for all four models as the time between clusters and number of feedings in a cluster were varied.

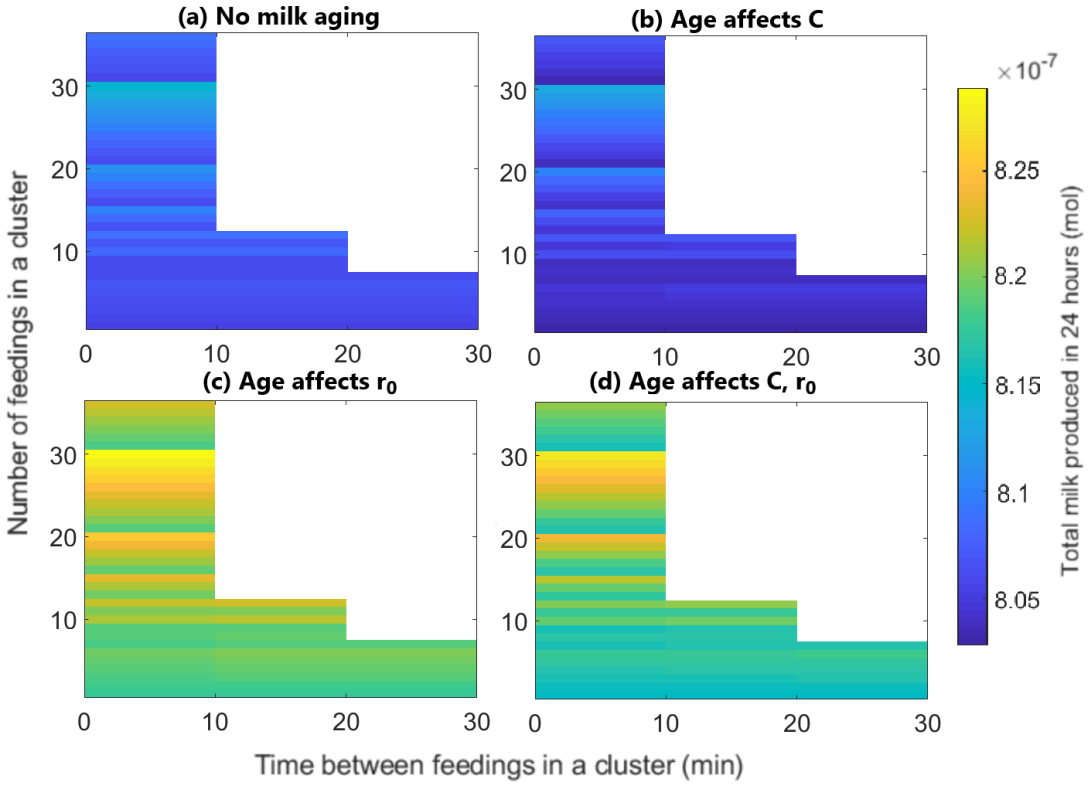

Figure 3.11: Total milk produced in 24 hours for each of the four versions of Model 1, with varied feeding schedules parameterized by the time between feedings in a single cluster (t_b) and the number of feedings in a cluster (N_c). The feeding schedule period was held fixed at 4 hours and the total amount of time spent feeding per period was fixed at one hour.

Each model shows a similar pattern: the time between feedings in cluster (t_b) does not noticeably affect the amount of milk produced while the number of feedings in a cluster (N_c) does change the amount of milk produced slightly. Although the variations in milk produced for each N_c seems random, the pattern persists across all models. Although this persistent, "random" pattern may be the result of coarse time-steps generating errors in approximating the feeding schedule, use of a smaller time step produced a similar pattern. Figure 3.12 shows the milk production for the final Model 1 version (aged milk affecting C and r_0) using a time-step of 0.01 min.

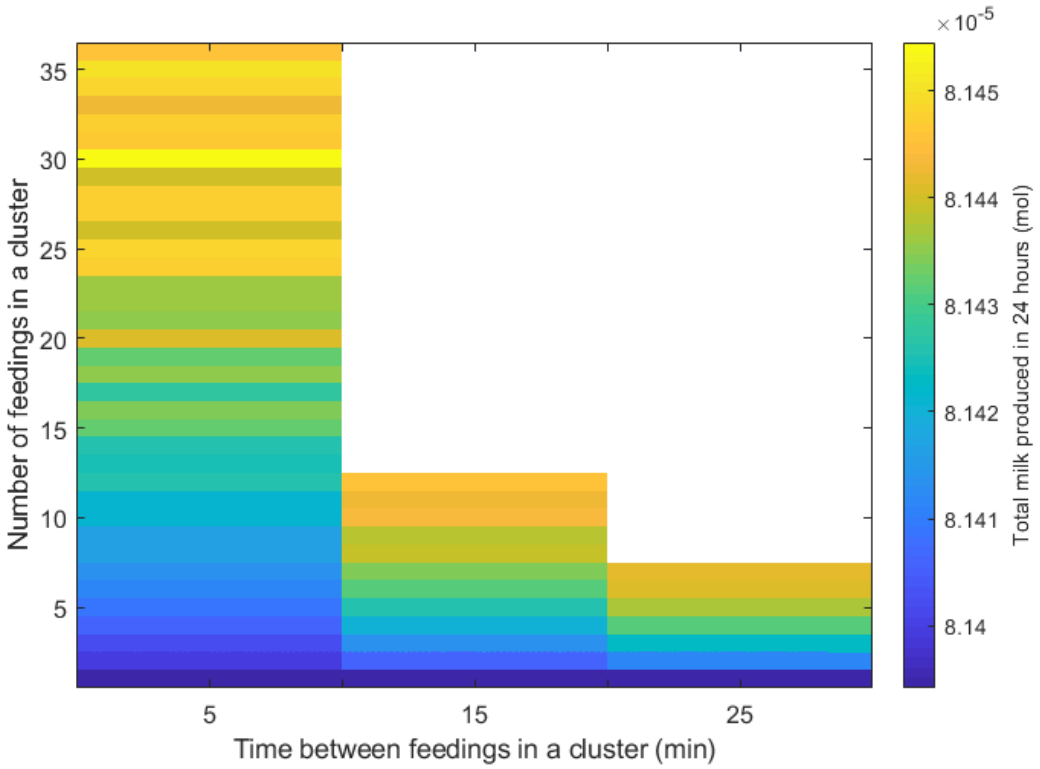

Figure 3.12: Total milk produced in 24 hours as predicted by Model 1 with aged milk affecting cell quiescence and alveolus size, and with varied feeding schedules parameterized by the time between feedings in a single cluster (t_b) and the number of feedings in a cluster (N_c). A smaller time-step of 0.01 min was used to reduce error in the feeding schedule approximation. The feeding schedule period was held fixed at 4 hours and the total amount of time spent feeding per period was fixed at one hour.

Refining the time-step smooths the pattern somewhat and distinguishes between the amount of milk produced between different times between feedings in a cluster. However, there are still drops in the amount of milk produced as N_c increases. It may be that the difference in milk production between one feeding schedule and the next is small enough that even very small errors in the feeding schedule approximation could lead to significant differences in the amount of milk produced. This could explain the persistent peaks at $N_c = 10$, 12, 15, 20 and 30, which all evenly divide 60 minutes. Due to substantial computation times, time steps smaller than 0.01 min were not

explored for this section. In order to determine what might cause the decreases in production, two similar feeding schedules were compared: $N_c = 20$ and $N_c = 21$, with $t_b = 5$ min used for both. Figure 3.13 shows sample days of milk production with these two feeding schedules.

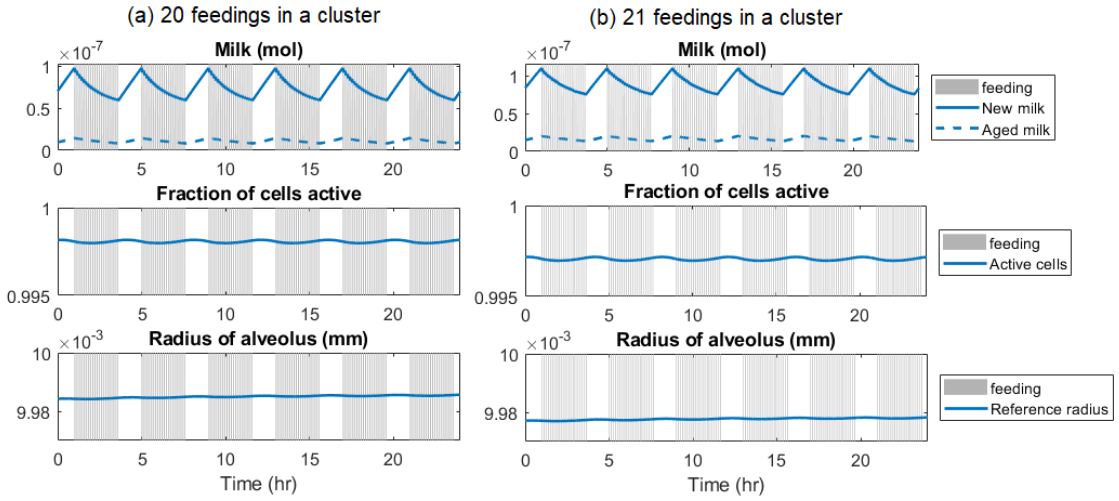

Figure 3.13: Simulated milk curve for 24 hours with Model 1, constant milk removal with aged milk affecting cell quiescence and alveolus size. Clusters of feeding occur every four hours with 5 minutes between feedings in a cluster, one hour of feeding total for each cluster and either (a) 20 or (b) 21 feedings in a cluster. Gray regions indicate time periods of feeding. With (a) 20 feedings in a cluster 8.2367×10^{-6} mol of milk is produced in these 24 hours, while with (b) 21 feedings in a cluster 8.1640×10^{-6} mol is produced.

With $N_c = 21$, both new and aged milk levels are consistently higher than with $N_c = 20$, which in turn causes both C and r_0 to be lower. Thus milk production is lower with 21 feedings in a cluster. The amount of time spent feeding is likely underestimated then—because new and aged milk levels are higher but the amount of milk produced is lower, less milk must be removed during feeding than with $N_c = 20$. With less milk removed, less milk is produced and the lactation system tends toward an equilibrium.

Overall, there is a general increase in milk production as the number of feedings in a cluster increases and as the time between feedings in a cluster increases. Taking

only values of N_c with $60 \bmod N_c = 0$, milk production strictly increases with the number of feedings per cluster. Increasing either N_c or t_b moves the feeding schedule closer to a regular feeding schedule (all feedings equally spaced) with a higher frequency of feeding than the original regular feeding schedule used.

3.2. Model 2: Pressure-based milk removal

In order to compare modeling a single alveolus to multiple alveoli, the flow rate of milk out of the alveoli must be based on the physics and geometry of the mammary gland rather than simply having a constant, prescribed flow rate. Section 2.2 describes how this flow rate is calculated for each case: a single alveolus and multiple alveoli. Because of the requirement of solving a non-linear equation or system of equations at each time-step, times for completely simulations are fairly slow, taking about 40 minutes to simulate 36 hours of lactation. For both cases, the final version of Model 1, constant milk removal with aged milk affecting both cell quiescence and alveolus size, was used to model milk production.

Flow out of a single alveolus

Before testing multiple alveoli, the behavior of the model with the new pressure-based milk removal was investigated. Using the same parameters from Model 1, as well as new, physical parameters for the fluid flow, one day of feeding regularly for one hour in every four was simulated. Figure 3.14 shows the simulated milk production for a day early in lactation onset while the alveolus is still growing.

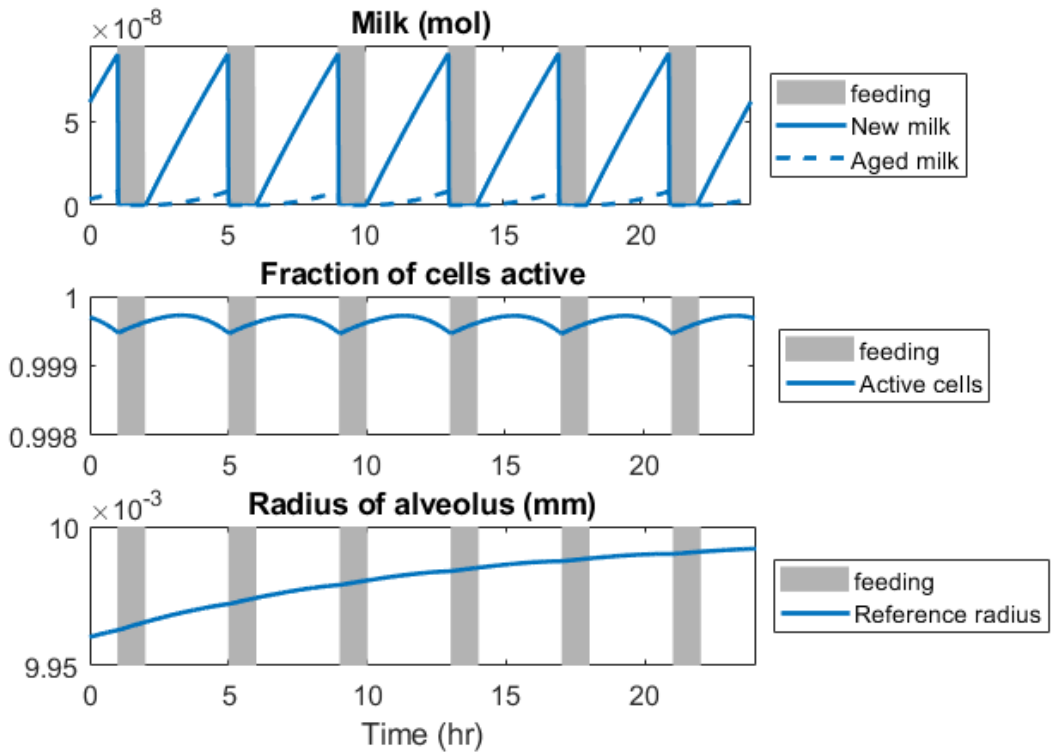

Figure 3.14: Simulated milk curve for 24 hours of feeding one hour in every four, with Model 2, pressure-based milk removal with a single alveolus. Gray regions indicate time periods of feeding.

Although new and aged milk oscillate similarly with constant or pressure-based removal, pressure-based removal necessarily led to emptying of the alveolus at each feeding. When parameters that may lead to slower milk removal were used, either the numeric solver (Matlab's `fsolve`) failed to solve Equation 3.7 (e.g., larger duct radius r_d or larger maximum reference radius $r_{0,max}$) or large changes in the parameter had little effect and did not prevent the alveolus from emptying (e.g., changing elastic modulus K of the alveolus wall or the pressure P_B of infant suckling). In this case, pressure build up inside the alveolus as well as oxytocin-induced contraction of the alveolus wall lead to immediate release of milk upon suckling, demonstrating the let-down reflex (Newton and Newton 1948).

The fraction of cells active oscillate near one, as in Model 1, with the same period. However, with aged milk low and removed immediately upon feeding, C is

consistently higher and experiences much sharper troughs in its oscillation. There is no smooth increase in C after feeding begins and milk is removed; instead C immediately increases upon the beginning of feeding and C spends more time increasing than decreasing. Although the alveolus reference radius is still growing, milk levels are so low due to the regular emptying of the alveolus that milk production is not significantly affected by the lowered reference radius. Because involution is characterized by the lack of feeding and because implementation of feeding is the difference between Models 1 and 2, involution will follow the same pattern in this model as in the final version of Model 1 and is not shown.

Different cluster feeding schedules were applied to this model and amounts of milk produced compared. To reduce computation time, the time-step was not refined further. Figure 3.15 shows the amount of milk produced in 24 hours for each cluster feeding schedule.

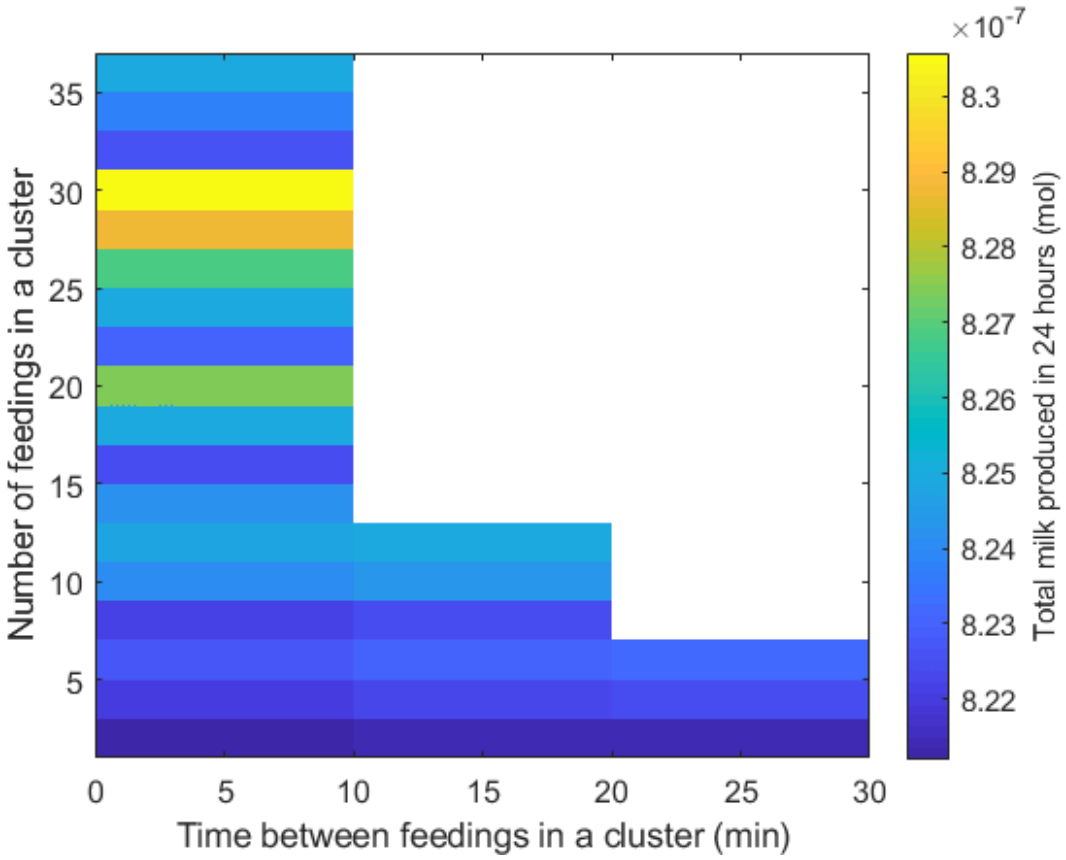

Figure 3.15: Total milk produced in 24 hours for each of the four versions of Model 2 in a single alveolus, with varied feeding schedules parameterized by the time between feedings in a single cluster (t_b) and the number of feedings in a cluster (N_c). The feeding schedule period was held fixed at 4 hours and the total amount of time spent feeding per period was fixed at one hour.

As in Model 1, milk production generally increases with more feedings in a cluster, with some sporadic decreases possibly caused by errors in approximating the feeding schedule. In this case, the time between feedings in a cluster has an effect even for the coarse time-step, with milk production increasing slightly as t_b increases. Increasing either N_c or t_b moves the feeding schedule closer to a regular feeding schedule (all feedings equally spaced) with a higher frequency of feeding than the original regular feeding schedule used.

Including pressure-based milk removal necessitates alveolus emptying and gen-

erates a system very sensitive to parameters describing the geometry of the simulated mammary gland. Additionally, increases in milk production with increasing time between feedings in a cluster were present, and therefore greater milk production in more regular and frequent feeding schedules.

Flow out of multiple alveoli

Although the number of alveoli in a mammary gland is far larger than three (in dogs, there can be as many as 3,000 alveoli), to save on computation time, three alveoli were modeled (Orfanou et al. 2010). The general geometry of the three alveoli was as shown in Figure 2.2. Each alveolus was 1 mm away from the main duct ($l_k = 1$ mm for $k = 1, 2, 3$) and the main duct was 6 mm long, with alveoli evenly spaced along the duct so that $l_{d,k} = 2$ mm for $k = 1, 2, 3$. All duct radii were equal with $r_k = r_{d,k} = 0.0005$ mm for $k = 1, 2, 3$ (larger duct radii caused `fsolve` to fail to solve Equations 3.9a-3.10c for the junction pressures $P_{J,k}$ and stretched alveolus radii $r_{A,k}$).

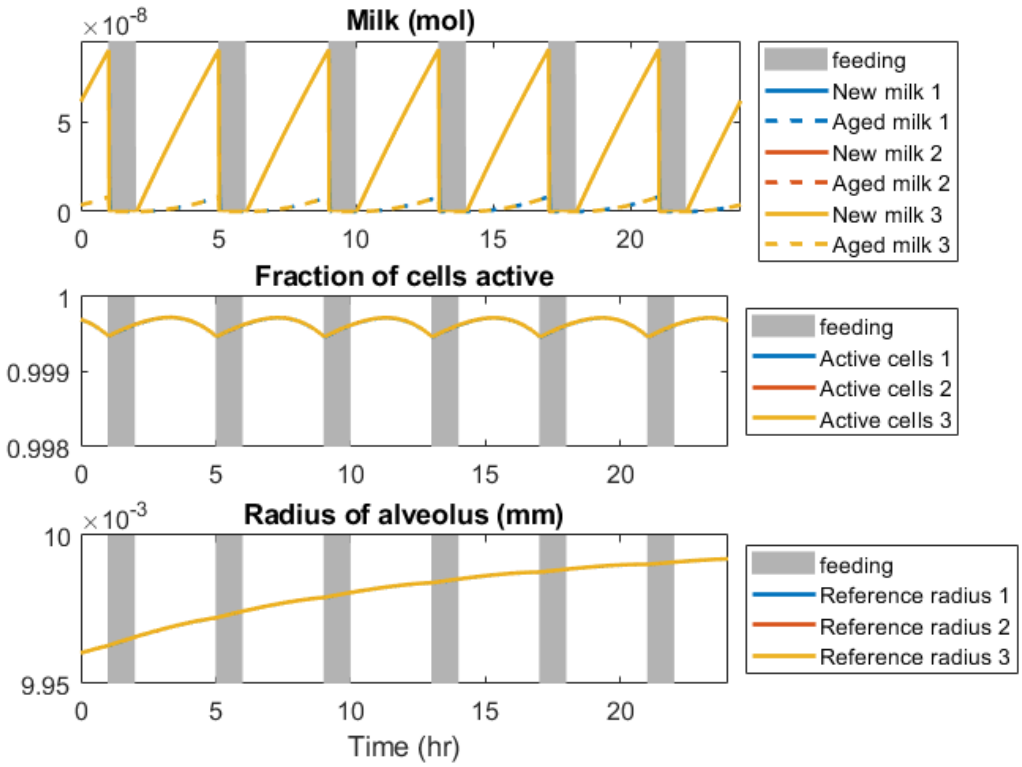

Figure 3.16: Simulated milk curve for 24 hours of feeding one hour in every four, with Model 2, pressure-based milk removal with three alveoli. Alveolus 1 is furthest from the nipple while alveolus 3 is closest. Gray regions indicate time periods of feeding.

Each of the three alveoli behave the exact same way, and behave the same as in the single alveolus case (Figure 3.14). Additional milk volume entering the main duct has not slowed milk removal or prevented the alveoli from emptying immediately upon feeding onset. Comparing the application of different feeding schedules shows similar patterns as well. Figure 3.17 shows the amount of milk produced in total for all three alveoli for different feeding schedules and a reduced number of sample values for N_c to save computation time.

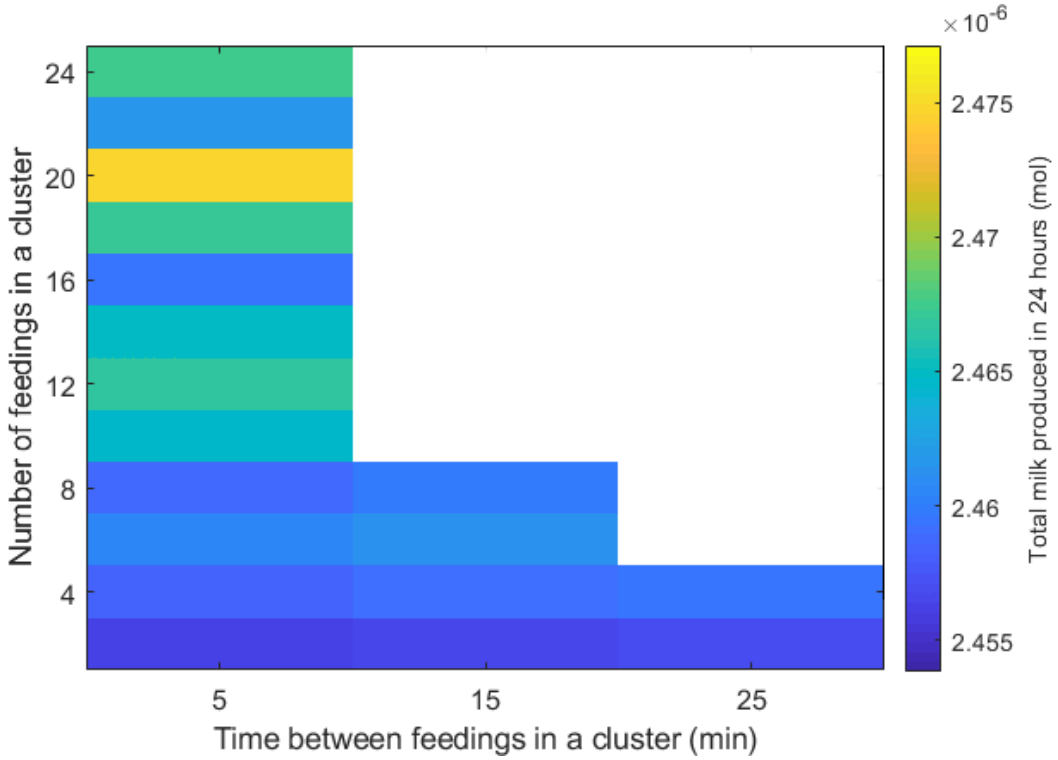

Figure 3.17: Total milk produced in 24 hours for each of the four versions of Model 2 in three alveoli, with varied feeding schedules parameterized by the time between feedings in a single cluster (t_b) and the number of feedings in a cluster (N_c). The feeding schedule period was held fixed at 4 hours and the total amount of time spent feeding per period was fixed at one hour.

With three alveoli instead of one, the total capacity for amount of milk produced is tripled and this is reflected in the amount of milk produced for each feeding schedule, which is about triple the amount produced in the single alveolus case (Figure 3.17). As with the single alveolus cases, the amount of milk produced generally increases as feedings become more frequent and regular (Figures 3.11, 3.15).

Although the dynamics of milk production are not noticeably different when modeling more alveoli, the amount of milk produced is greater with multiple alveoli. In Figure 3.16 the total amount of milk produced in the displayed 24 hours is 2.455×10^{-6} mol. To compare, a single alveolus was simulated with a maximum volume equal to the total maximum volume of three alveoli ($r_{0,max} = 0.01 \cdot 3^{1/3}$ mm for the single

alveolus and $r_{0,max} = 0.01$ mm for the three alveoli). The single alveolus produced 1.706×10^{-6} mol in 24 hours, about 2/3 of the amount produced with three alveoli. Because r_0^2 directly affects the milk production rate (Equation 2.1b), but also affects the amount of stretch experienced by an alveolus, as well as the pressure P_k inside the alveolus, the amount of milk produced is dependent upon alveolus surface area as well as alveolus volume. Thus modeling more alveoli allows for greater surface area and greater milk production.

Because the alveoli were emptied immediately upon feeding in both the single alveolus and multiple alveolus cases, each of the three alveoli are exact copies of each other and demonstrate no change in the dynamics of milk production. In order to see a noticeable difference between alveoli, the distance between alveoli along the main duct needs to be large: $l_{d,k} = 30$ mm. Figure 3.18 shows a day of regular feeding with three alveoli each 30 mm apart.

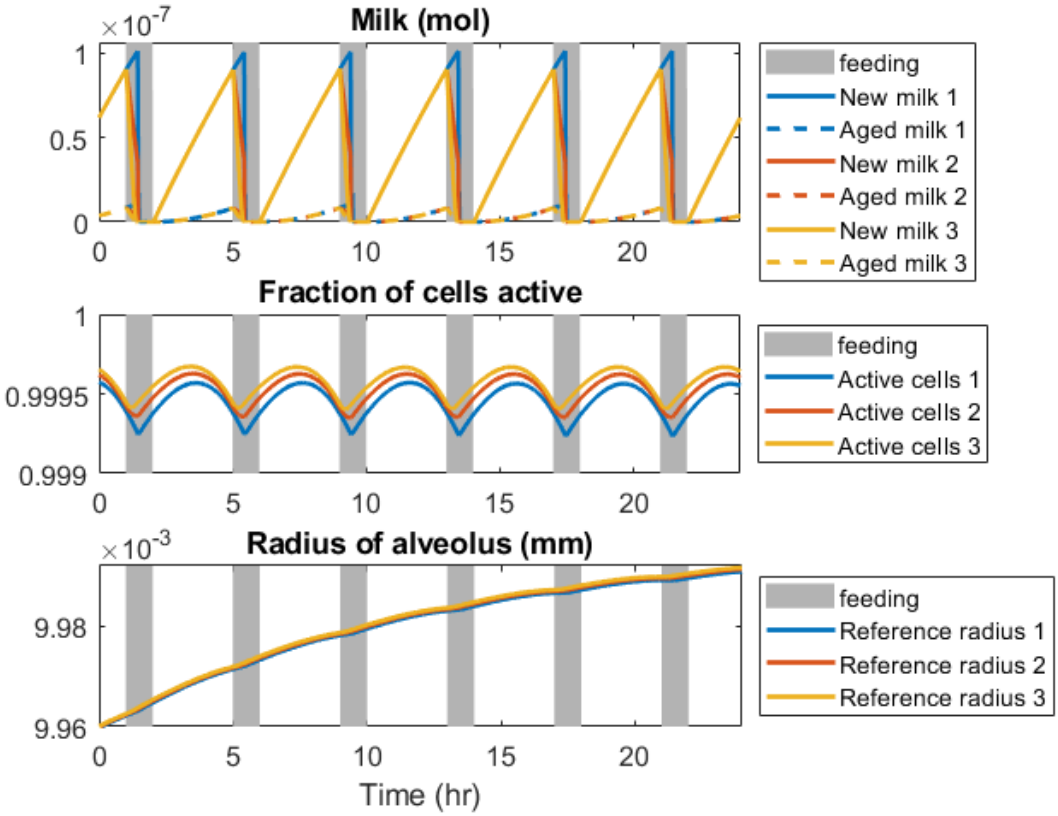

Figure 3.18: Simulated milk curve for 24 hours of feeding one hour in every four, with Model 2, pressure-based milk removal with three alveoli. Alveolus 1 is furthest from the nipple while alveolus 3 is closest, with $l_d = 30$ mm between each alveolus along the main duct. Gray regions indicate time periods of feeding.

Increasing the distance between alveoli to 30 mm causes the alveolus closest to the nipple (alveolus 3, shown in yellow) to empty faster. Alveolus 1 (blue), the furthest from the nipple, continues to gain milk at the onset of feeding until both the closer alveoli are emptied. The fractions of cells active and alveoli reference radii are now noticeably different between alveoli, but only very slightly. As milk is being produced between feedings, the alveoli are producing milk seemingly identically, and it is only once feeding begins that there alveoli become distinct, suggesting that the small changes to C and r_0 between alveoli are not large enough to significantly affect milk production. It is possible that even longer, less physiological, duct lengths could

allow for greater differentiation between alveoli, but this would necessitate folding of the duct in order for it to fit inside the mammary gland and imaging of the breast does not show this kind of structure (Ramsay et al. 2005).

4. Discussion

4.1. Model 1: Constant milk removal

With Model 1, two different local effects for aged milk were explored: aged milk deactivating alveolar cells and aged milk causing alveolar cell death. These two effects, together and separately, did not noticeably change the daily milk patterns and caused only minor changes to the pattern of involution. Although including the effects of aged milk on production did cause new milk to level off fairly quickly after feeding ended in the first stage of involution, aged milk continued to rise rapidly. Thus the total amount of milk, new and aged, still rose rapidly throughout the first stage of involution. However, the marked loss of productive cells due to milk aging, either by quiescence or apoptosis of alveolar cells, is a key marker of the first stage of involution (Watson 2006; Geddes 2007; Schere-Levy et al. 2003). While the different aging effects did not necessarily change how total milk levels behaved during involution, both milk aging effects captured a key hallmark of involution stage one (Figures 3.1-3.9).

The main difference between the aging effects was the total amount of milk produced in 24 hours (Figures 3.10-3.12). Because when the fraction of alveolar cells active C was not changing with aged milk C was held constant at one, allowing C to change could only decrease the alveolus' capacity for milk production. Thus including the effect of aged milk on the fraction of cells active always decreased the total amount of milk produced. The alveolus reference radius, however, was set below its maximum when not changing with aged milk. Thus allowing the reference radius to change meant the alveolus could grow as well as shrink, and the capacity for milk production could increase. Thus holding both C and r_0 at their maximums when they were not changing would mean that both could cause decreases in milk production when allowed to change with aged milk.

These particular values were chosen to best match the cases in which each variable would not be affected by aged milk. If the fraction of cells active is not

affected by aged milk and quiescent cell activation is not a method of modulating milk production, then the presence of quiescent/stem cells likely do not influence the production capacity of a single alveolus, although they may cells may be activated or deactivated in order to change the total number of alveoli (Hassiotou and Geddes 2013; Orfanou et al. 2010). For simplicity, it was then assumed that in these cases the fraction of active cells was one. If the reference radius of the alveolus is not affected by aged milk, then there must be some other method of changing alveolus size because alveoli can change size throughout lactation (Orfanou et al. 2010). Because we are interested in the low milk production case and methods of increasing production, it was assumed that alveoli were not at their maximum size. Using different assumptions or considering different cases would allow milk production to either increase or decrease with the addition of aged milk effects. Further research into the dynamics of mammary cells during lactation is needed to determine which assumptions are most relevant when considering mothers with low production.

Milk aging could affect milk production through either of the considered mechanisms. Both were capable of affecting milk production and both exhibited similar dynamics. Additionally both mechanisms are equally capable of explaining how insufficient breast drainage and prolonged periods between feedings could decrease milk production. If milk aging causes mammary cells to deactivate, then accumulation of aged milk—from either insufficient milk drainage during feeding or prolonged absence of feeding—would cause alveolar cells to become quiescent and stop producing milk until enough aged milk could be removed to allow quiescent cells to be re-activated. If milk aging causes mammary cell apoptosis, then accumulation of aged milk would cause milk-producing cells to die, thereby decreasing the capacity for production until enough aged milk could be removed to decrease the cell death rate and allow the cell population to increase. Because both aged milk effects were found to be biologically feasible and to reproduce known lactation dynamics equally well, both effects were used in Model 2.

4.2. Model 2: Pressure-based milk removal

Including fluid dynamics and pressure-based milk removal into feeding with Model 2 allowed for the exploration of the effects of the geometry of the mammary gland on milk production. This model, however, was very sensitive to certain parameters, in particular the radius of the ducts $r_{d,k}$, and seemed to have little to no dependence on other parameters, most notably the pressure of infant suckling P_B.

Under this restrictive parameter regime, the alveoli always empty during feeding (Figures 3.14, 3.16, 3.18). This forced emptying generated sharper troughs in the oscillations of the fraction of cells active, and prevented any differences in milk production from emerging. When multiple alveoli were simulated, they were then more like copies of the single alveolus case rather than a separate model to consider. Extending the duct length beyond what is physiologically realistic may allow for new patterns to emerge. Additionally, modeling more alveoli, allowing for a more complex geometry, may reveal differences in milk production between alveoli and would be a more realistic model to use for investigating low milk production.

The mammary gland could be approximated as a single large alveolus rather than many small alveoli, and this approximation was used when initially creating Model 1. However, collecting the volume of all the alveoli in the breast together into a single larger alveolus reduces milk production capacity. As discussed in section 3.2, milk production depends upon alveolus surface area as well as volume, so increasing the total amount of surface area in the mammary gland allows for higher milk production. This may be why the mammary gland evolved a structure more similar to the lungs, with many small alveoli, than the stomach, with one large sac. One large sac is energetically less expensive to develop—fewer cells need to be made and kept up, and it is easier to deliver nutrients to each cell with blood vessels. The fact that mammals have evolved branched mammary gland structures with many alveoli suggests that high milk production in mothers is essential to the success of mammalian offspring.

4.3. Increasing milk production

Because low milk production has become an issue for many women, methods of increasing production must be found and changing the feeding schedule has been proposed as a solution (Kent et al. 2012; Daly et al. 1996). Using the models presented, we were able to determine that increased frequency of feeding does increase milk production. Additionally, more time feeding also increases the amount of milk produced. Splitting a single feeding into a cluster of multiple feedings did increase production, but production increased further if those feedings were spaced out and no longer clustered. Therefore cluster feeding can cause an increase in milk production, but only through the increase in the number of feedings in a day. The optimal feeding schedule seems to be feeding as frequently, as regularly and as much as possible (Figures 3.11, 3.12, 3.15 and 3.17).

Unfortunately, the most frequent feeding schedules examined in Figures 3.11, 3.12, 3.15 and 3.17 are incredibly unrealistic for any human being. Feeding for two minutes every five minutes is impractical and does not allow for much time to doing anything other than feeding—if the infant can even be convinced to feed in those two minutes. This "optimal" feeding schedule is then not really optimal and could not reasonably be suggested as a method for increasing milk production. In order to determine and truly optimal feeding schedule, many other components of infant growth and health would need to be included, such as sleep. Cluster feeding may be a way to increase the number of feedings in a day while still allowing time for both mother and infant to do other things.

4.4. Future work

In order to fully explore the presented models, more alveoli could to be simulated. This model could also be combined with a model similar to the fluid dynamics model of the breast by Negin Mortazavi et al. (2016). With a more complete simulation of the actual mammary gland, new milk production patterns may emerge, and the feeding schedules tested may have a different effect on production.

This model could also be paired with existing metabolism models, like the model by Hall (2006), to track infant growth throughout lactation. Such a model could

explore the effects of hunger and compare infant growth between the infant demand feeding schedule and more regular feeding schedules. If combined with circadian rhythm and sleep models, the development of a normal (adult-like) sleep cycle could be studied.

Although the reasons why low milk production is common in developed countries is unknown, factors like stress are known to affect milk production (Dewey 2001). Other biological signalling molecules are also known to affect lactation, including TRH, serotonin, insulin and insulin-like growth factor (IGF) (Lemay et al. 2013; van de Moosdijk et al. 2017; Horseman and Collier 2013). Model 1 could be modified to include these factors in order to investigate possible causes of low milk production, and therefore possible pharmacological interventions.

Because not all physical and biological components of lactation were included, this model cannot describe lactation as a whole. However, for investigating the effects of different feeding schedules on milk production, the presented models balance simplicity with predictive power and greater complexity is not necessary.

References

Amis, D. 2015. A Childbirth Educators Commentary on Hormonal Physiology of Childbearing: Evidence and Implications for Women, Babies, and Maternity Care . The Journal of Perinatal Education, 24(3):154–159. [Cited on page 1.]

Bertram, R., Egli, M., Toporikova, N., and Freeman, M. E. 2006. A mathematical model for the mating-induced prolactin rhythm of female rats. American Journal of Physiology-Endocrinology and Metabolism, 290(3):573–582. [Cited on page 5.]

Buckley, S. J. 2015. Executive Summary of Hormonal Physiology of Childbearing: Evidence and Implications for Women, Babies, and Maternity Care. The Journal of Perinatal Education, 24(3):145–153. [Cited on page 1.]

Cox, D. B., Owens, R. A., and Hartmann, P. E. 1996. Blood and milk prolactin and the rate of milk synthesis in women. Experimental Physiology, 81(6):1007–1020. [Cited on pages 3 and 4.]

Dag, B., Keskin, I., and Mikailsoy, F. 2005. Application of different models to the lactation curves of unimproved Awassi ewes in Turkey. South African Journal of Animal Sciences, 35(4):238–243. [Cited on page 2.]

Daly, S., Owens, R., and Hartmann, P. 1993. The shortterm synthesis and infantregulated removal of milk in lactating women. Experimental Physiology, 78(2):209–220. [Cited on page 3.]

Daly, S. E., Kent, J. C., Owens, R. A., and Hartmann, P. E. 1996. Frequency and degree of milk removal and the short-term control of human milk synthesis. Experimental Physiology, 81(5):861–875. [Cited on pages 1, 3, 26, and 44.]

Dewey, K. G. 2001. Maternal and fetal stress are associated with impaired lactogenesis in humans. The Journal of nutrition, 131(11):3012S–5S. [Cited on pages 1 and 45.]

Dijkstra, J., France, J., Dhanoa, M., Maas, J., Hanigan, M., Rook, A., and Beever, D. 2010. A Model to Describe Growth Patterns of the Mammary Gland During Pregnancy and Lactation. Journal of Dairy Science, 80(10):2340–2354. [Cited on pages 2 and 4.]

Egli, M., Leeners, B., and Kruger, T. H. 2010. Prolactin secretion patterns: Basic mechanisms and clinical implications for reproduction. Reproduction, 140(5):643–654. [Cited on page 2.]

Ferreira, A. G., Henrique, D. S., Vieira, R. A., Maeda, E. M., and Valotto, A. A. 2015. Fitting mathematical models to lactation curves from holstein cows in the southwestern region of the state of Parana, Brazil. Anais da Academia Brasileira de Ciencias, 87(1):503–518. [Cited on page 2.]

Fewtrell, M. S., Kennedy, K., Ahluwalia, J. S., Nicholl, R., Lucas, A., and Burton, P. 2016. Predictors of expressed breast milk volume in mothers expressing milk for their preterm infant. Archives of Disease in Childhood: Fetal and Neonatal Edition, 101(6). [Cited on pages 1 and 26.]

Geddes, D. T. 2007. Inside the Lactating Breast: The Latest Anatomy Research. Journal of Midwifery and Women's Health, 52(6):556–563. [Cited on page 41.]

Grattan, D. R. 2015. 60 YEARS OF NEUROENDOCRINOLOGY: The hypothalamo-prolactin axis. Journal of Endocrinology, 226(2):T101–T122. [Cited on page 2.]

Hall, K. D. 2006. Computational model of in vivo human energy metabolism during semistarvation and refeeding. American Journal of Physiology-Endocrinology and Metabolism, 291(1):E23–E37. [Cited on page 44.]

Hassiotou, F. and Geddes, D. 2013. Anatomy of the human mammary gland: Current status of knowledge. Clinical Anatomy, 26(1):29–48. [Cited on page 42.]

Horseman, N. D. and Collier, R. J. 2013. Serotonin: A Local Regulator in the Mammary Gland Epithelium. Annual Review of Animal Biosciences, 2(1):353–374. [Cited on pages 8, 9, and 45.]

Hurst, N. M. 2007. Recognizing and Treating Delayed or Failed Lactogenesis II. Journal of Midwifery and Women's Health, 52(6):588–594. [Cited on page 1.]

Jenness, R. 1979. The composition of human milk. Seminars in perinatology, 3(3):225–239. [Cited on page 17.]

Jiang, H. and Sun, S. X. 2013. Cellular pressure and volume regulation and implications for cell mechanics. Biophysical Journal, 105(3):609–619. [Cited on page 11.]

Jindal, S., Gao, D., Bell, P., Albrektsen, G., Edgerton, S. M., Ambrosone, C. B., Thor, A. D., Borges, V. F., and Schedin, P. 2014. Postpartum breast involution reveals regression of secretory lobules mediated by tissue-remodeling. Breast Cancer Research, 16(2):1–14. [Cited on page 19.]

Kent, J. C. 2006. Volume and Frequency of Breastfeedings and Fat Content of Breast Milk Throughout the Day. Pediatrics, 117(3):e387–e395. [Cited on page 17.]

Kent, J. C., Prime, D. K., and Garbin, C. P. 2012. Principles for Maintaining or Increasing Breast Milk Production. Journal of Obstetric, Gynecologic, and Neonatal Nursing, 41(1):114–121. [Cited on pages 1, 3, and 44.]

Lemay, D. G., Ballard, O. A., Hughes, M. A., Morrow, A. L., Horseman, N. D., and Nommsen-Rivers, L. A. 2013. RNA Sequencing of the Human Milk Fat Layer Transcriptome Reveals Distinct Gene Expression Profiles at Three Stages of Lactation. PLoS ONE, 8(7). [Cited on page 45.]

Marasco, L. A. 2015. Unsolved Mysteries of the Human Mammary Gland: Defining and Redefining the Critical Questions from the Lactation Consultants Perspective. Journal of Mammary Gland Biology and Neoplasia, 19(3-4):271–288. [Cited on page 1.]

Mathworks, C. 2019. Function Reference R 2019 a. [Cited on pages 12 and 14.]

Negin Mortazavi, S., Geddes, D., and Hassanipour, F. 2016. Lactation in the Human Breast From a Fluid Dynamics Point of View. Journal of Biomechanical Engineering, 139(1):011009. [Cited on pages 2 and 44.]

Newton, M. and Newton, N. R. 1948. The let-down reflex in human lactation. The Journal of Pediatrics. [Cited on pages 11 and 32.]

Orfanou, D. C., Pourlis, A., Ververidis, H. N., Mavrogianni, V. S., Taitzoglou, I. A., and Boscos, C. M. 2010. Histological Features in the Mammary Glands of Female Dogs throughout Lactation. pages 473–478. [Cited on pages 35 and 42.]

Ramsay, D. T., Kent, J. C., Hartmann, R. A., and Hartmann, P. E. 2005. Anatomy of the lactating human breast redefined with ultrasound imaging. Journal of Anatomy, 206(6):525–534. [Cited on page 40.]

Rattanakul, C. and Lenbury, Y. 2009. A mathematical model of prolactin secretion: Effects of dopamine and thyrotropin-releasing hormone. Mathematical and Computer Modelling, 49(9-10):1883–1892. [Cited on page 5.]

Schere-Levy, C., Buggiano, V., Quaglino, A., Gattelli, A., Cirio, M. C., Piazzon, I., Vanzulli, S., and Kordon, E. C. 2003. Leukemia inhibitory factor induces apoptosis of the mammary epithelial cells and participates in mouse mammary gland involution. Experimental Cell Research. [Cited on pages 3, 8, and 41.]

Schmitt-Ney, M., Happ, B., Hofer, P., Hynes, N. E., and Groner, B. 2014. Mammary gland-specific nuclear factor activity is positively regulated by lactogenic hormones and negatively by milk stasis. Molecular Endocrinology, 6(12):1988–1997. [Cited on pages 3 and 8.]

Sunarić, S., Jovanović, T., Spasić, A., Denić, M., and Kocić, G. 2016. Comparative Analysis of the Physicochemical Parameters of Breast Milk, Starter Infant Formulas and Commercial Cow Milks in Serbia. Acta Facultatis Medicae Naissensis, 33(2):101–108. [Cited on pages 10 and 51.]

Tay, C. C., Glasier, A. F., and McNeilly, A. S. 1996. Twenty-four hour patterns of prolactin secretion during lactation and the relationship to suckling and the resumption of fertility in breast-feeding women. Human Reproduction, 11(5):950–955. [Cited on pages 2, 6, and 7.]

van de Moosdijk, A., Fu, N., Rios, A., Visvader, J., and Van Amerongen, R. 2017. Lineage Tracing of Mammary Stem and Progenitor Cells., volume 1501. [Cited on page 45.]

Walker, S. P. 1997. Nutritional issues for women in developing countries. Proceedings of the Nutrition Society, 56(1B):345–356. [Cited on page 1.]

Watson, C. J. 2006. Key stages in mammary gland development Involution: Apoptosis and tissue remodelling that convert the mammary gland from milk factory to a quiescent organ. Breast Cancer Research, 8(2):1–5. [Cited on pages 3, 19, and 41.]

Wilde, C. J. and Peaker, M. 1990. Autocrine control in milk secretion. The Journal of Agricultural Science, 114(3):235–238. [Cited on pages 3, 6, and 8.]

Wood, P. 1968. Factors affecting persistency of lactation in cattle. Nature, 218:894. [Cited on page 2.]

A. Parameter Values

Parameter	Value used	Description
R	8.31441 J/K/mol	Ideal gas constant
T	310 K	Body temperature
ν	2.4×10^{-3} MPa·s	Viscosity of milk (Sunarić et al. 2016)

Table A.1: Milk production model physical constants. These values were not changed throughout the model development process.

Parameter	Value used	Parameter	Value used
k_{P1}	1 min^{-1}	k_{P2}	0.5
k_{P3}	2 min^{-1}	k_{D1}	0.25 min^{-1}
k_{D2}	0.75	k_{D3}	0.5
k_{D4}	0.66 min^{-1}	k_{D5}	2.5 min^{-1}
k_U	1	k_{S1}	1 MPa^{-1}
k_{S2}	16.5 MPa	k_σ	1 MPa/mol
$k_{\omega 1}$	1 min^{-1}	$k_{\omega 2}$	1 min^{-1}
k_N	10^{-5} $\text{mol/mm}^2\text{/min}$	k_l	0.0001 min^{-1}
k_{Fl}	0.2 min^{-1}	k_G	0.001 min^{-1}
k_{C1}	0.01 min^{-1}	k_{C2}	10^3 $\text{mol}^{-1}\text{min}^{-1}$
k_{r1}	2 $\text{mm}^{-2}\text{min}^{-1}$	k_{r2}	1 $\text{mm}^{-2}\text{min}^{-1}$
$r_{0,max}$ *	0.01 mm	k_{r3}	700 $\text{mol}^{-1}\text{min}^{-1}$
l_d,$l_{d,k}$,l_k *	1 mm	r_d,$r_{d,k}$,r_k	0.0005 mm
K	100 MPa	h	0.0005 mm
$k_{P\omega}$	2×10^{-9} MPa	P_B (P_{baby})	0.001 MPa
β	1	Π_C	0.000625 mol/mm^3
N_c *	1	t_b *	20 min
Δt *	1 min		

Table A.2: Milk production model parameters. See Model chapter for description of parameters. These parameters were modified throughout the model development process and final parameter values were chosen based on whether simulations run with these parameters produced physiologically reasonable results. Parameters with a star (*) indicate those that were changed for tests shown in this thesis. Further discussion of parameter choices is included in the Model, Results and Discussion chapters.